

Division of Solid Mechanics

ISRN LUTFD2/TFHF--04/5107--SE (1-67)

A BIOMECHANICAL STUDY OF TISSUE FORMATION

Master's Dissertation by

Sandra Kotai

Supervisors

Ingrid Svensson, Div. of Solid Mechanics

Magnus Tägil, Dep. of Orthopaedics, Lund University Hospital

Ian McCarthy, Biomechanics Laboratory, Dep. of Orthopaedics, Lund
University Hospital

Copyright © 2004 by Div. of Solid Mechanics, Sandra Kotai
Printed by KFS AB, Lund, Sweden.

For information, address:
Division of Solid Mechanics, Lund University, Box 118, SE-221 00 Lund, Sweden.
Homepage: <http://www.solid.lth.se>

Acknowledgment

This master thesis has been carried out at the Division of Solid Mechanics, Department of Mechanical Engineering at Lund Institute of Technology in collaboration with the Department of Orthopedics at Lund University Hospital.

I wish especially to thank my supervisors Dr. Ingrid Svensson at the Division of Solid Mechanics, Dr. Magnus Tägil and Dr Ian McCarthy at the Department of Orthopedics for their guidance and support, which has helped me a lot through the work.

Finally thank you everyone that has helped and supported me during this work.

Lund, April 2004

Sandra Kotai

Abstract

The objective of this thesis is to investigate how the mechanical environment of healing tissue influences the tissue formation. Tägil et al [2] made an experimental study of the mechanical control of tissue differentiation in vivo at the Biomechanical Laboratory at Lund University Hospital. In that study a bone chamber was designed and implanted in the tibia of a group of rats. After 3 weeks, when tissue had grown up into the empty bone chamber, it was mechanically loaded during another 7 weeks. The result from that study is compared with the finite element analyses of the tissue within the chamber. To decide which type of tissue that formed, two mechanobiologic hypotheses and a fuzzy logic model have been tested. The hypotheses were proposed by Carter et al [7] and Claes et al [3]. In Carters hypothesis an osteogenic factor is introduced, expressed in terms of principal stresses. In Claes hypothesis quantitative boundaries have been given in order to predict whether cartilage, bone or connective tissue will be formed, depending on the amount of hydrostatic pressure and strains the tissue experience. The fuzzy logic model is proposed by Hofer et al [10] and is based on the concept of a modified osteogenic factor and a degree of membership. The results from the analyses with Carters hypothesis and Hofers model were similar to the results from the experiment, but the result from the analysis with Claes hypothesis did not correlate so well. In a future experiment with the bone chamber different values of applied load at the top are suggested, to get a better verification of the results from the finite element analyses. The value of the pressure is recommended to be below 2MPa, which was used in the experiment. Further the bone chamber should be harvested at several different points of time, which is needed to get more detailed information of the course of events during the time of loading.

Contents

1	Introduction.....	1
1.1	Background.....	1
1.2	Objective and restrictions	1
2	Medical issues.....	3
2.1	The anatomy of bone	3
2.2	Cartilage.....	5
2.3	The process of bone growth.....	5
2.3.1	Intramembranous ossification.....	5
2.3.2	Endochondral ossification.....	6
2.4	The process of fracture healing.....	6
2.4.1	Secondary healing.....	6
3	Theory.....	9
4	The bone chamber experiment.....	11
5	Methods to describe the correlation between loading and tissue differentiation..	13
5.1	Hypothesis by Carter.....	13
5.2	Hypothesis by Claes.....	15
5.3	Fuzzy logic model by Hofer	16
5.3.1	Identification of the tissue composition.....	17
5.3.2	Calculation of stimuli.....	17
5.3.3	The Fuzzy controller	18
5.3.3.1	Fuzzyfication.....	18
5.3.3.2	The fuzzy rules.....	18
5.3.3.3	Defuzzyfication.....	20
5.3.4	Calculation of a new tissue composition	21
6	Models.....	23
6.1	The three-dimensional finite element model	24
6.1.1	Loading and boundary conditions.....	25
6.2	The two-dimensional finite element model	27
6.2.1	Loading and boundary conditions.....	28
7	Results.....	29
7.1	Carters hypothesis.....	29
7.2	Claes hypothesis.....	32
7.3	Fuzzy logic model by Hofer	34
8	Discussion and future work.....	37
	References.....	39

Appendix A	41
Some medical expressions often used in the thesis	41
Appendix B	43
Criterion by Drucker-Prager	43
Appendix C	45
Matlab Code	45
Hypotheses by Carter and Claes	45
Fuzzy logic model by Hofer	51

Chapter 1

Introduction

This master thesis has been carried out at the Division of Solid Mechanics, Department of Mechanical Engineering at Lund Institute of Technology in collaboration with the Department of Orthopedics at Lund University Hospital. It is the final assignment of my education at the Mechanical Engineering program at Lund Institute of Technology.

1.1 Background

There are a number of factors which influences the mechanical environment at the fracture site in terms of interfragmentary strain. The loads applied and the characteristics of the fixation device are maybe the most important. The relation between the levels of strain induced at the fracture site and the progression of healing, in that only certain types of tissue can exist in areas of specific strain magnitude, is complex.

Primary fracture healing, i.e. the fracture healing by direct bone filling of the fracture gap without the intermediary phase of cartilage formation, is rare. It only exists when a fracture is rigidly fixed surgically and interfragmentary strain is minimal. Secondary healing is the most common healing process when fractures heal spontaneously or are stabilized by various forms of external fixation or intramedullary nailing. In this healing process the fragments are stabilized by the formation of periosteal callus. Initially, the fracture gap is occupied by the fracture haematoma, which differentiates through granulation tissue, fibrous tissue and fibrocartilage to woven and lamellar bone. Each of these tissues have different mechanical properties optimized for the mechanical environment. The stiffness increases with the advance from granulation tissue to bone, whereas the ultimate tensile strain decreases. Therefore, the interfragmentary movement is reduced as healing progresses. However, the progression to the next tissue is impeded or the tissue is damaged, if the loads across a healing fracture are too large. A lack of sufficient stability can lead to a non-union with excessive periosteal hard callus and a cartilaginous endpoint at the fracture line.

An understanding of the general relationship between specific biological tissues and the mechanical environment is essential for the future development of orthopedic implants and treatment methods for fractures [1].

1.2 Objective and restrictions

Tägil et al [2] made an experimental study of the mechanical control of tissue differentiation in vivo at the Biomechanical Laboratory at Lund University hospital. In that study a bone chamber was designed and implanted in the tibia of a group of rats.

After 3 weeks, when tissue had grown up into the empty bone chamber, it was mechanically loaded during another 7 weeks. The result from that study is compared with the finite element analyses of the tissue within the chamber. The objective of this thesis is to investigate how the mechanical environment of healing tissue, influences the tissue formation. The main tasks of the thesis are

- Study of medical and biomechanical literature to understand the medical issues involved in tissue formation and find tissue differentiation models.
- Create finite element models with the bone chamber experiment as basis.
- Implementation of the medical models of tissue formation and differentiation into finite element models.
- Evaluate the finite element models.

Since the study of tissue differentiation is a complex problem, the fluid flow acting within the tissue has not been considered.

Chapter 2

Medical issues

In this chapter the architecture and function of bone and cartilage are described. For further information about bone and cartilage the reader is referred to [1,3,4,5,6]. The language used in biomechanical literature is different from what a mechanical engineer is used to. In Appendix A some of the medical terms used in the thesis are explained.

2.1 The anatomy of bone

Bone is the stiffest tissue and the main component of the skeleton in the adult human. There are three major types of bone cells; osteoblasts, osteoclasts and osteocytes. The osteoblasts are the surface bone forming cells, whereas the osteoclasts resorb bone. The osteocytes are embedded in the bone matrix and function as modulator of the formation and resorption by sensing strain. At the macroscopic level there are two types of bone; compact and cancellous bone. Compact bone, is a dense material whereas cancellous bone has a spongy appearance. Cancellous bone, also called trabecular bone, is composed of short struts of bone tissue called trabeculae [3] forming a sandwich construction whereas cortical bone is more like a tube with thicker walls. Compact bone is mainly found in the diaphysis of the long bones, whereas cancellous bone makes up the meta- and epiphysis of the long bone, see Figure 2.1.

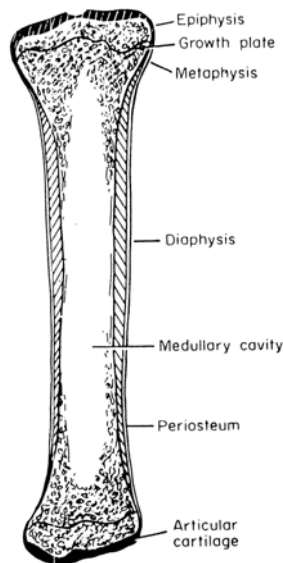


Figure 2.1: Long bone.

At the microscopic level three types of compact bone can be seen; woven, lamellar and haversian. Woven bone is a bone type with random orientation formed early in a healing bone or when no load is sensed by the bone. The osteoblasts deposit the matrix in compact bone, in thin sheets which are called lamellae. Lamellar bone is bone composed of lamellae when viewed under the microscope. A majority of the individual lamellae in compact bone form concentric rings around larger canals (approx. 50 μm in diameter) called the haversian canals within the bone tissue. The haversian canals and surrounding lamellae are called haversian systems. Haversian bone consists of these haversian systems. The basic structure of compact bone can be seen in Figure 2.2.

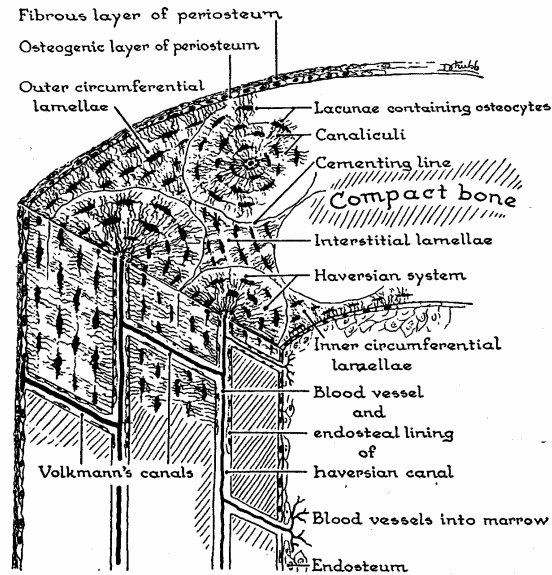


Figure 2.2: The structure of compact bone.

Cancellous bone does not form haversian systems. It is made up of a series of interconnecting plates perforated by holes [1], see Figure 2.3 below.

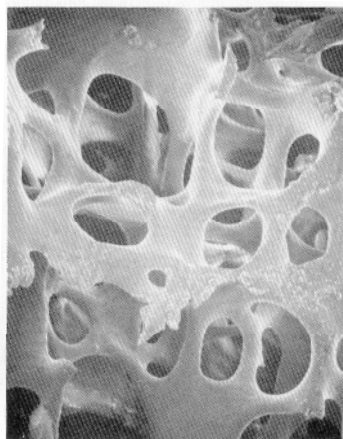


Figure 2.3: The structure of cancellous bone.

2.2 Cartilage

Cartilage is a specialized type of connective tissue and does not contain vessels or nerves. It is formed by chondroblasts and resorbed by chondroclasts. Three different kinds of cartilage can form due to the mechanical environment; hyaline cartilage, elastic cartilage and fibrous cartilage, see Figure 2.4. The most common is hyaline cartilage which is found in the nose, larynx and joints. Hyaline cartilage is nearly transparent and is blue shimmering in the colour with thin, collagen fibers, which do not appear because they have about the same refractive index as the matrix. This leads to the vitreous appearance of the hyaline cartilage [4]. Elastic cartilage is found in the external ear and corresponds histological to hyaline cartilage, but in addition, it contains a dense network of fine branched elastic fibers. Fibrous cartilage is found in the discs of the spine and contains a large number of collagen fibers and a very small amount of matrix.

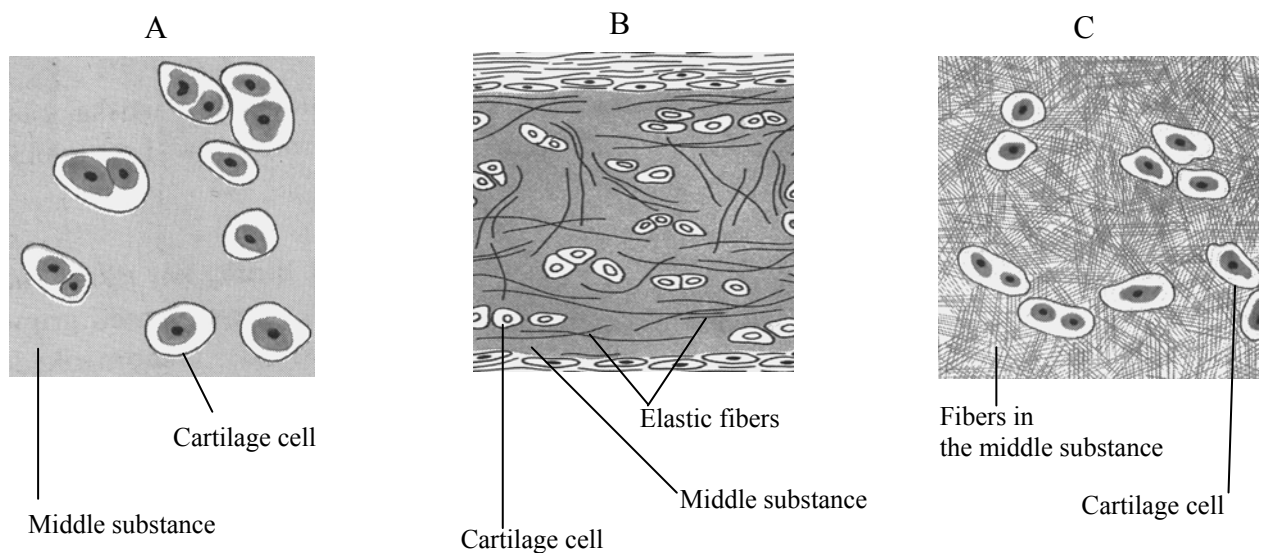


Figure 2.4: (A) Hyaline cartilage; (B) Elastic cartilage; (C) Fibrous cartilage.

2.3 The process of bone growth

Two mechanisms of bone formation can be distinguished due to the mechanical environment of the healing tissue; intramembranous ossification and endochondral ossification.

2.3.1 Intramembranous ossification

Intramembranous ossification refers to the growth of bones, in mechanically less loaded bone such as the frontal and parietal bones of the skull [5]. The process takes place within an embryonic tissue membrane through the apposition of bone on tissue. Membrane-like

layers of connective tissue are provided with dense networks of blood vessels, which attract the connective tissue cells. These cells increase in size and differentiate into osteoblasts. The osteoblasts then deposit osteoid and mineralize it to create a matrix of trabecular bone. Outside the periosteum lie the cells of the primitive connective tissue. The cells produce a layer of compact bone to cover the surface of newly formed trabecular bone [5].

2.3.2 Endochondral ossification

The majority of bones in the skeleton grow through the process of endochondral ossification. In this process the deformations are too large for bone to survive and the final bone is preceded by cartilage more apt to harvest the initial deformations. Ribs, vertebrae, the cranial base and bones of the extremities begin as cartilage models in an environment in which the function of support is less necessary. Blood vessels infiltrate the center of the diaphysis within the cartilage model and ossification take place. This region is called the primary ossification center. The cartilage model is surrounded by a thin membrane called perichondrium. Osteoblastic progenitor cells produce osteoblasts in this region. The osteoblasts deposit a thin layer of compact bone around the primary ossification center. The diameter of the diaphysis is increasing when the resulting periosteum continues to deposit bone layer upon layer. With this increase, osteoclasts on the endosteal surface, the inner side of the bone tube, resorb bone while osteoblasts on the periosteal, outer surface deposit bone. Thus appositional growth allows diaphyseal diameter to increase and the medullary canal to develop [5].

2.4 The process of fracture healing

Healing begins as undifferentiated mesenchymal cells migrate from the surroundings and produce initial connective tissue around the fracture site, forming an initial stabilizing callus. The development of the callus is influenced by the size of the fracture gap and by the amount of mechanical stability. There are two major processes of fracture healing: primary healing and secondary healing. Primary healing occurs in cases of extreme stability and negligible gap size [6]. However, most cases, which involve moderate gap sizes and fracture stability, heal by secondary fracture healing [6]. The process of primary healing is slow and takes months or years to complete, whereas secondary healing is relatively rapid, with bony union achieved in weeks to months [1]. The process of secondary healing is described in Chapter 2.4.1

2.4.1 Secondary healing

In the process of secondary healing mesenchymal cells differentiate into cartilage and bone forming cells, which leads to the formation of cartilage and bone tissue in the callus. In successful secondary healing the initial connective tissue and cartilage are entirely replaced by bone, leading to osseous union across the fracture gap and completion of the healing process. Consider an intact long bone, see Figure 2.5.

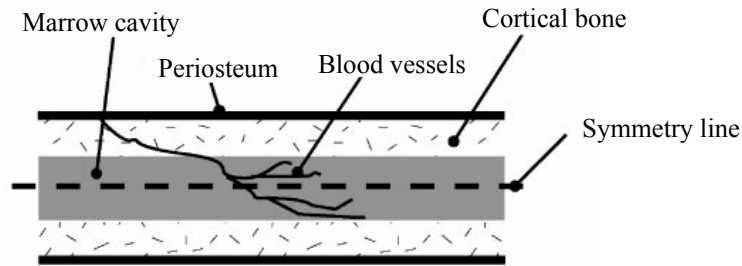


Figure 2.5: Schematic of a section through an intact long bone.

The fracture healing process can be divided into four stages; inflammation, callus differentiation, ossification and remodeling (see Figure 2.6). Immediately after the bone fracture, when blood quickly fills the fracture gap space, an inflammatory reaction starts. A connective tissue matrix consisting of fibrin is created by platelets and thrombotic factors. White blood cells migrate to the fracture site and promote the formation of a matrix, necessary for the migration of mesenchymal cells, which originate from surrounding tissues. These cells replace the fibrin matrix by a new connective tissue matrix and form the initial callus [6].

In the second stage of fracture healing, bone and cartilage is formed in distinct regions of the callus. Along the bone, within the first 24 hours, mesenchymal cells differentiate into osteoblasts which begin to create intramembranous woven bone. In the interior of the initial callus and adjacent to the fracture, at approximately day 7, mesenchymal cell differentiate into chondrocytes which create cartilage. As healing progresses the intramembranous ossification front advances towards the center of the callus until 10-12 days of healing and the chondrous callus grows in size.

Now the third healing stage of the soft tissue starts. Endochondral ossification continues until all cartilage has been replaced by bone and an entirely bony bridge closes the fracture gap [6]. Once the gap has ossified and the fracture is stable, the fourth stage of repair begins lasting for several years. It ends with the restoration of the original form of the bone

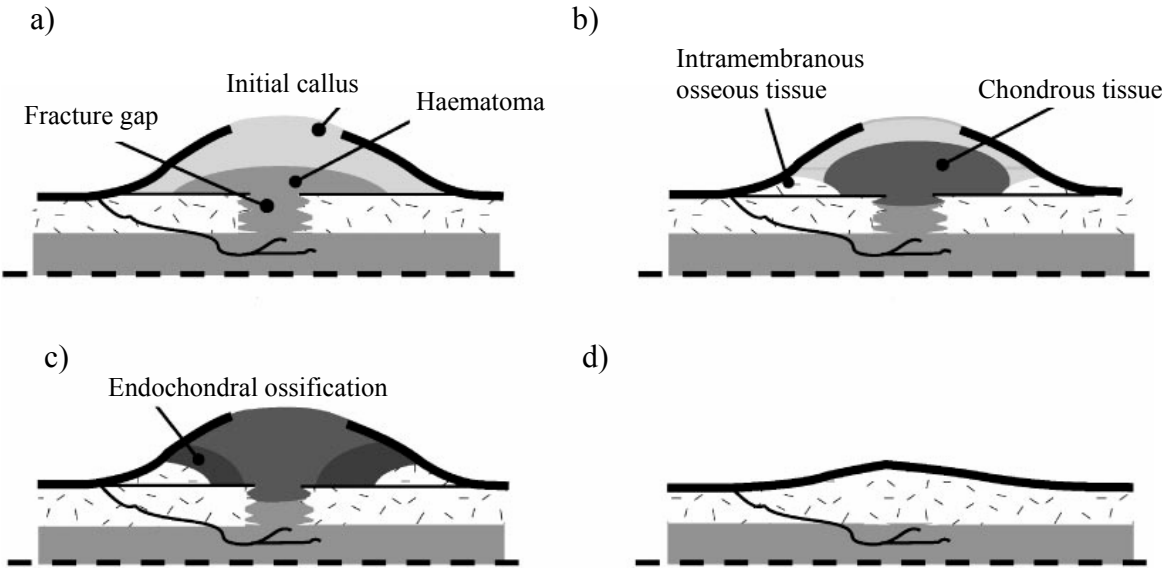


Figure 2.6: The fracture healing stages of an intact long bone:
 a) the first stage, inflammation ; b) the second stage, differentiation of callus;
 c) the third stage, ossification; d) the fourth stage, remodeling.

Chapter 3

Theory

The hypothesis proposed by Carter et al [7] uses two stress invariants: octahedral shear stress and hydrostatic stress. In this chapter the octahedral shear stress and hydrostatic stress are introduced.

In a principal stress direction, the shear stresses are equal to zero. Further, the principal stress directions are always orthogonal. A plane with a normal that makes equal angles to the three principal stress directions is defined as an octahedral plane [8], see Figure 3.1. The three principal stress directions are here denoted by 1, 2 and 3.

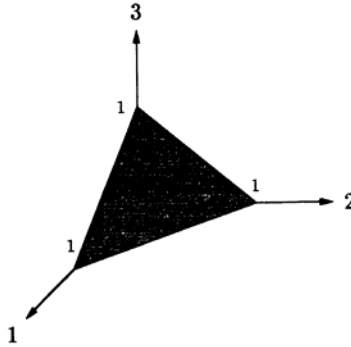


Figure 3.1: The octahedral plane.

The unit vector to the octahedral plane in Figure 3.1 is given by

$$\mathbf{n} = \frac{1}{\sqrt{3}} \begin{bmatrix} 1 \\ 1 \\ 1 \end{bmatrix} \quad (3.1)$$

If a coordinate system collinear with the principal stress directions is chosen the stress tensor takes the form

$$\boldsymbol{\sigma} = \begin{bmatrix} \sigma_1 & 0 & 0 \\ 0 & \sigma_2 & 0 \\ 0 & 0 & \sigma_3 \end{bmatrix} \quad (3.2)$$

Consider a surface with the outer normal unit vector \mathbf{n} . The traction vector \mathbf{t} acting on the surface is defined as

$$\mathbf{t} = \boldsymbol{\sigma} \mathbf{n} \quad (3.3)$$

The traction vector can always be resolved into one component parallel to \mathbf{n} and one component perpendicular to \mathbf{n} . The component parallel to \mathbf{n} is called the normal stress in direction \mathbf{n} and denoted by σ_n . From Equation 3.3 it follows that

$$\sigma_n = \mathbf{n}^T \mathbf{t} = \mathbf{n}^T \boldsymbol{\sigma} \mathbf{n} \quad (3.4)$$

The component of \mathbf{t} perpendicular to \mathbf{n} is called the shear stress and is defined as

$$\tau_n = \mathbf{m}^T \mathbf{t} = \mathbf{m}^T \boldsymbol{\sigma} \mathbf{n} \quad (3.5)$$

where the unit vector \mathbf{m} is perpendicular to \mathbf{n} and located in the plane ABCD, illustrated in Figure 3.2.

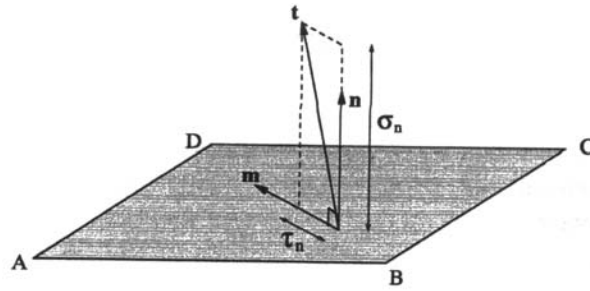


Figure 3.2: The normal stress σ_n and shear stress τ_n .

With Equations 3.1 and 3.2 it then follows that the normal stress and tensorial shear stress on the octahedral plane are given by

$$\sigma_o = \frac{1}{3} I_1 ; \quad \tau_o = \sqrt{\frac{2}{3} J_2} \quad (3.6)$$

where σ_o is called the octahedral normal stress or hydrostatic stress and τ_o is called the octahedral shear stress. I_1 and J_2 are the stress invariants. In index notation they read as

$$\begin{aligned} I_1 &= \sigma_{ii} \\ J_2 &= \frac{1}{2} s_{ij} s_{ij} \end{aligned} \quad (3.7)$$

where σ_{ij} is the stress tensor and s_{ij} is the deviatoric stress tensor given by

$$s_{ij} = \sigma_{ij} - \frac{1}{3} \sigma_{kk} \delta_{ij} \quad (3.8)$$

Note that an invariant always takes the same value irrespective of the coordinate system. For further information the reader is referred to [8].

Chapter 4

The bone chamber experiment

Tägil et al [2] made an experimental study of the mechanical control of tissue differentiation in vivo at the Biomechanical Laboratory at Lund University Hospital. To perform the study a bone chamber was designed and implanted in the tibia of a group of rats. The bone chamber consists of two threaded titanium half cylinders held together by a cap. The interior of the chamber has a diameter of 2 mm, and a length of 7 mm. At the bottom of the chamber there are two bone in-growth openings where tissue can grow into the chamber, which is empty from the beginning, see Figure 4.2a.



Figure 4.1: The bone chamber.

The loading device consists of a 1.8-mm-diameter piston and a spring, see Figure 4.2b. When a force (F) is applied on the top, the piston (P) protrudes into the chamber, and the tissue (C) within the chamber is mechanical loaded. The piston returns to its original position by means of the spring (S) when loading is interrupted, leading to no further mechanical stimuli acting on the tissue.

One end of the implant was screwed into the bone, the rat tibia. The chamber was then unloaded for 3 weeks, allowing tissue to grow into the empty chamber through the two in-growth openings, see Figure 4.2a. The tissue within the chamber contained three different zones. At the bottom there was a zone with cancellous bone, with a marrow cavity. Higher up there was more immature woven bone. Above this frontier there was a zone of fibrous tissue (soft tissue). Subsequently load was applied by hand on the top of the chamber, during 3 seconds followed by an unloaded interval of another 3 seconds. This 6-second-cycle was repeated 20 times, twice a day.

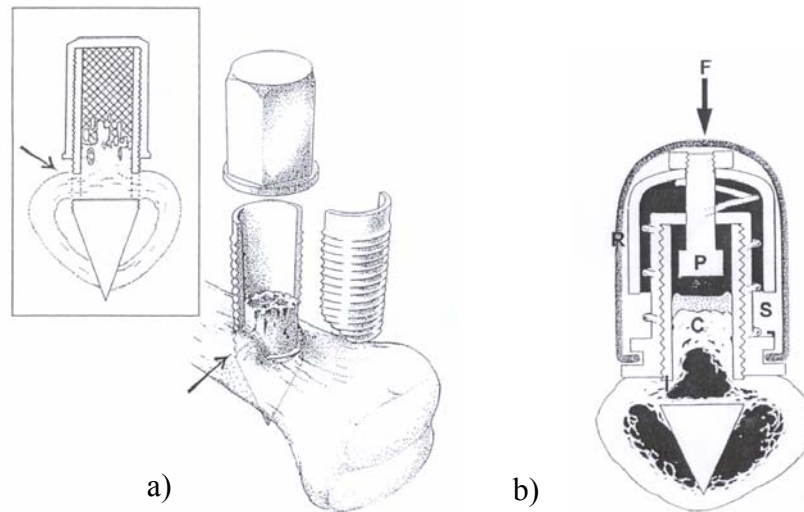


Figure 4.2: Sketches of the bone chamber:
 a) Arrows point at in-growth openings. b) The loading device.

The loading was estimated to produce a compressive hydrostatic stress of 2 MPa. After 7 weeks of loading, the chambers, which all contained newly formed bone, were harvested. Cartilage was then found next to the piston.

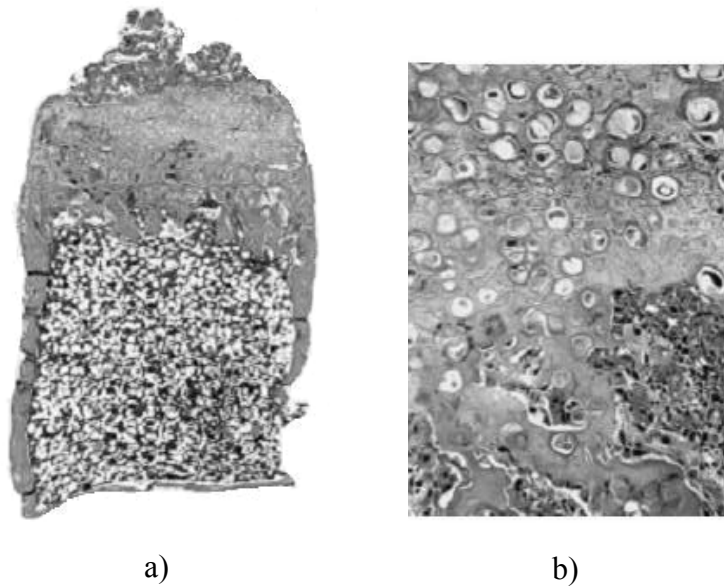


Figure 4.3: Tissue specimen from one of the bone chambers after 7 weeks of loading.

- a) A layer of cartilage has formed on the top next to the loading piston. Beneath the cartilage layer there is a bone plate followed by a marrow cavity at the bottom.
- b) Detail of induced cartilage, where the cartilage cells look like rolled oats.

Chapter 5

Methods to describe the correlation between loading and tissue differentiation

To simulate the experiment described in Chapter 4, finite element analyzes were performed with the two models described in Chapter 6. The two hypotheses and the fuzzy logic model presented in this chapter were used to decide whether cartilage will form due to the mechanical loading situation or not.

5.1 Hypothesis by Carter

Carter et al [7] studied the correlations between mechanical stress history and tissue differentiation in initial fracture healing. A finite element analysis was performed with two-dimensional models of a healing osteotomy in a long bone. In the study it was suggested that high compressive hydrostatic stresses encourage the transformation from connective tissue into cartilage. An osteogenic index I was introduced, reflecting the tendency for ossification. A low value of the osteogenic index reflects the prediction of cartilage and a high value indicates formation of bone or fibrous tissue. The osteogenic index is given by

$$I = \sum_{i=1}^c n_i (S_i + kD_i) \quad (5.1)$$

where the subscript i indicates a specific loading case, n_i = number of loading cycles, S_i = cyclic octahedral shear stress, D_i = cyclic hydrostatic (dilatational) stress, and k = empirical constant to be determined. With $c = 1$ and $n_1 = 1$, Equation 5.1 is reformulated into

$$I = S + kD \quad (5.2)$$

The shear octahedral stress S , and the dilatational or hydrostatic stress D , are given by

$$\begin{aligned} S &= \left(\frac{1}{3}\right) \sqrt{(\sigma_1 - \sigma_2)^2 + (\sigma_2 - \sigma_3)^2 + (\sigma_3 - \sigma_1)^2} \\ D &= \left(\frac{1}{3}\right) (\sigma_1 + \sigma_2 + \sigma_3) \end{aligned} \quad (5.3)$$

where σ_1, σ_2 and σ_3 are the peak principal stresses.

A schematic view of the hypothesis is presented in Figure 5.1. The hypothesis has been plotted in the SD-plane i.e. Equation 5.2 is rewritten on the form

$$S = I - kD \quad (5.4)$$

If there is poor vascularity within the tissue there are three different regions represented in the SD-plane; cartilage, bone and fibrous tissue, see Figure 5.1a. With good vascularity there will only be two regions, i.e. there is no region of bone represented in the SD-plane, see Figure 5.1b. The vascularity of the tissue inside the bone chamber is supposed to be in somewhere between poor and bad.

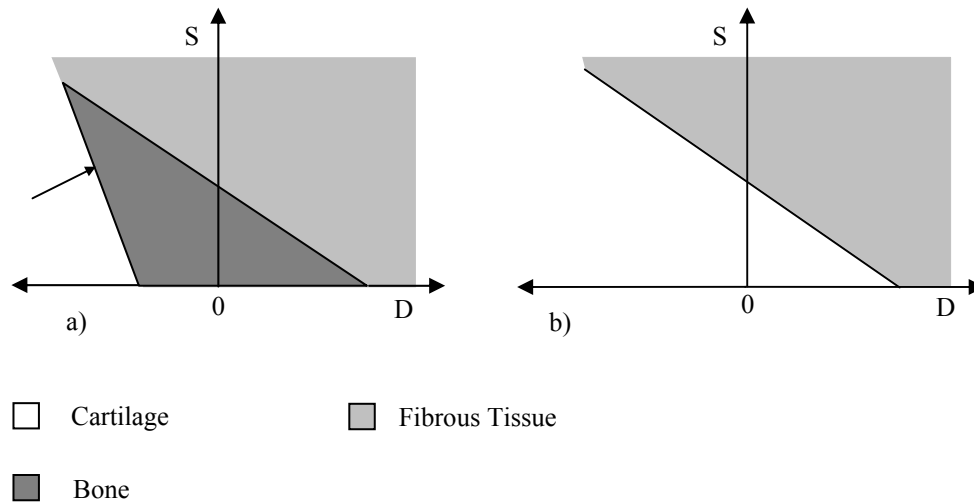


Figure 5.1: Carters hypothesis: a) Good vascularity; b) Poor vascularity.
The arrow in (a) points at the straight line, which divides the regions of cartilage and bone.

The slope and position of the two straight lines, which can be seen in Figure 5.1a, have to be identified before any conclusion can be drawn, whether cartilage, bone or fibrous tissue will be formed. In this thesis fibrous tissue is not considered and consequently the straight line which divides the region of bone from the region of fibrous tissue has not been identified in this thesis. The slope of the straight line corresponds to the negative empirical constant in Equation 5.4. The slope and position of the line gives the reference value for the osteogenic index. The reference value serves as a threshold value for determining whether bone or cartilage will form. An osteogenic index which exceeds the reference value leads to prediction of bone, whereas an osteogenic index below the reference value predicts cartilage. If the slope of the line and the value of the dilatational stress where the line intersects with the D-axis are known, the reference value for the osteogenic index can be calculated with Equation 5.2.

It seems that there is an analogy between the initial yield criteria proposed by Drucker and Prager [8] and the hypotheses of tissue differentiation proposed by Carter et al [7], see Appendix B.

5.2 Hypothesis by Claes

The hypothesis proposed by Claes et al [9], related the local tissue formation in a fracture gap to the local stress and strain. In their study the results from a finite element model were compared with histological findings from an animal fracture model. They suggested that the differentiation of the callus tissue is determined by the size of the strains and hydrostatic pressure along existing calcified surfaces in the fracture callus. For compressive pressures larger than about -0.15 MPa and strains smaller than $\pm 15\%$ the hypothesis predict endochondral ossification, in which bone is preceded by cartilage. Intramembranous ossification is predicted for strains smaller than approximately $\pm 5\%$ and hydrostatic pressure smaller than ± 15 MPa. Strains and stresses which do not fulfill the conditions stated above leads to connective tissue or fibrous cartilage. A graphical interpretation of the hypothesis is shown in Figure 5.2. In the regions denoted by A and B, bone respectively cartilage is predicted. Connective tissue/fibrocartilage is indicated in the region termed C.

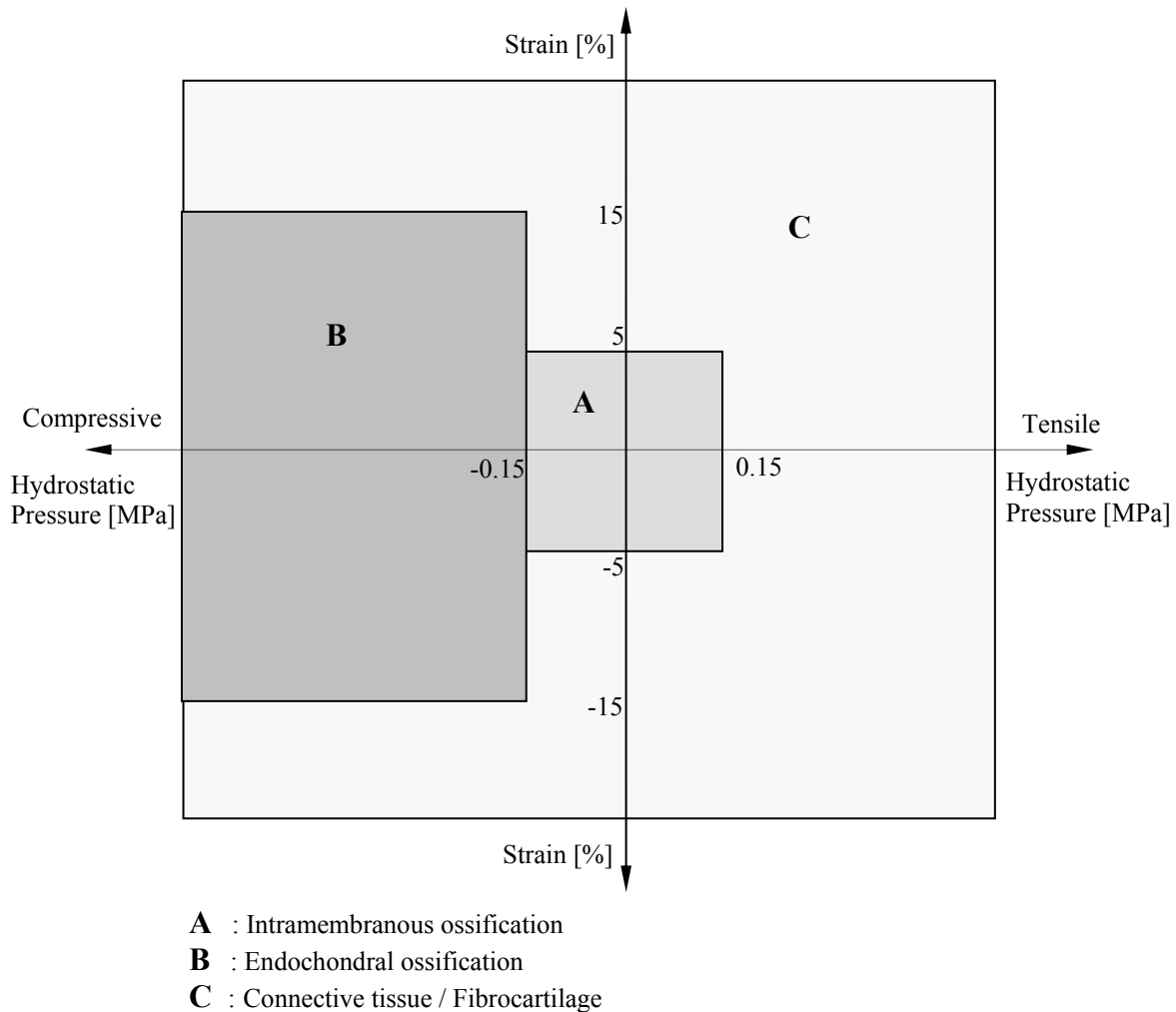


Figure 5.2: Schematic view of Claes hypothesis.

5.3 Fuzzy logic model by Hofer

Hofer et al [10] made a biomechanical model, which describe the tissue transformation during fracture healing of a sheep metatarsal. The model uses fuzzy logic and a feed back signal to predict the tissue repair. Three types of tissue are distinguished in the model; bone, cartilage and fibrous connective tissue. The soft tissue that initial was found in the bone chamber experiment described in Chapter 4 is a type of fibrous connective tissue. For simplification fibrous connective tissue will be termed as connective tissue in this chapter. In Figure 5.3 the feedback regulation system is presented, which shows the procedure for the calculations. The system can be divided into four parts; “identification of the tissue composition”, “calculation of stimuli”, “the fuzzy controller” and “calculation of a new tissue composition”.

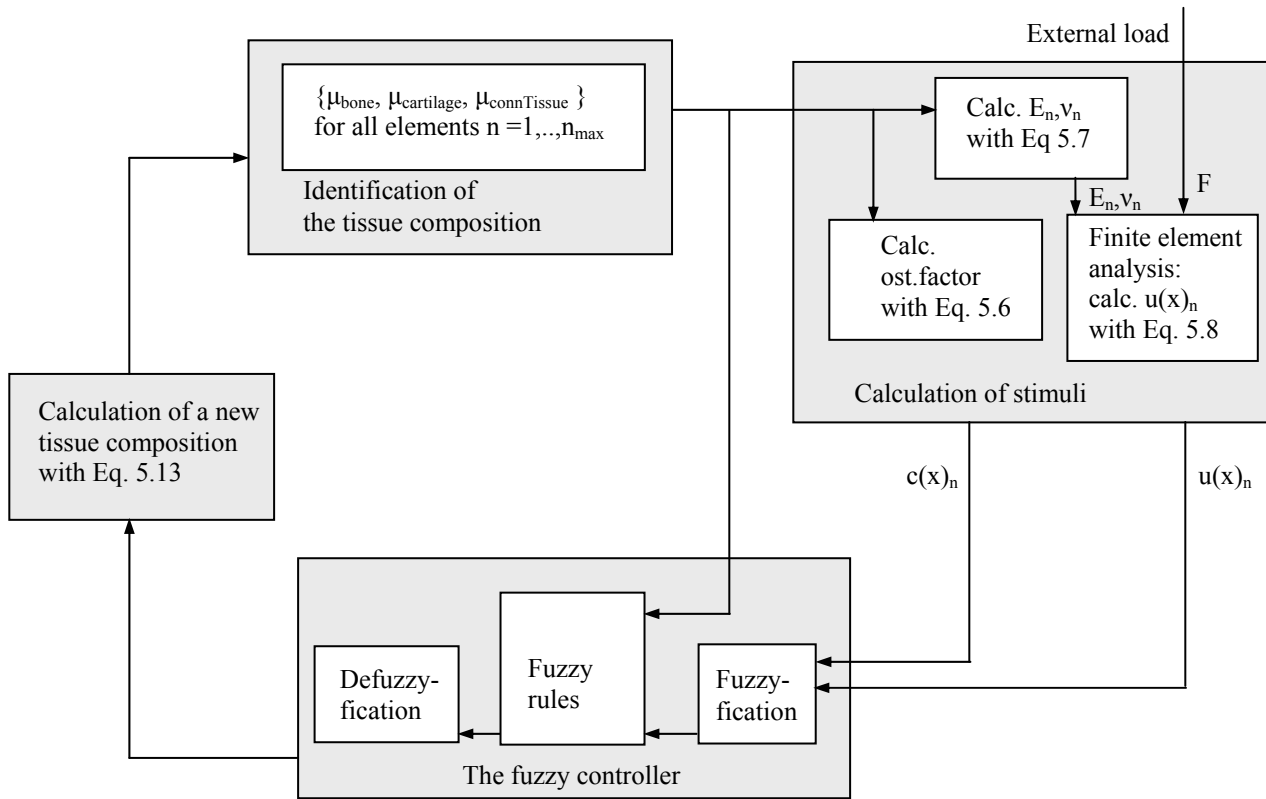


Figure 5.3: The feedback regulation system of the fuzzy logic model.

5.3.1 Identification of the tissue composition

The tissue composition of the element is defined by the degree of membership for bone (μ_{Bone}), cartilage ($\mu_{\text{Cartilage}}$) and connective tissue ($\mu_{\text{ConnTissue}}$), which varies between 0 and 1 continuously. For example, if one element consists of 50 % bone, 25% cartilage and 25% connective tissue the degrees of membership read as

$$\{\mu_{\text{Bone}} = 0.5, \mu_{\text{Cartilage}} = 0.25, \mu_{\text{ConnTissue}} = 0.25\}$$

For every elements the following balance equation must be satisfied

$$\mu_{\text{Bone}} + \mu_{\text{Cartilage}} + \mu_{\text{ConnTissue}} = 1 \quad (5.5)$$

This is under the assumption that each element is completely composed by the three different types of tissue discussed previously. In the first loop the tissue composition is given by the initial state. In the next following loops the tissue composition is obtained through the last part of the loop, which is described in Chapter 5.3.4.

5.3.2 Calculation of stimuli

The osteogenic factor $c(x)$ is given as the absolute value of the derivative of the degree of membership.

$$c(x) = \left| \frac{\partial \mu_{\text{Bone}}(x)}{\partial x} \right| \quad (5.6)$$

The osteogenic factor is calculated for every element in the finite element model. Note that this definition of the osteogenic factor is different from the one introduced by Carter et al [7]. All the tissues are assumed to be isotropic and linear elastic. For the determination of the Young's modulus E and the Poisson's ratio ν a mixture rule is applied. It uses a weighted sum of the material properties of the three types of tissue.

$$\begin{aligned} E &= E_{\text{Bone}} \cdot \mu_{\text{Bone}} + E_{\text{Cartilage}} \cdot \mu_{\text{Cartilage}} + E_{\text{ConnTissue}} \cdot \mu_{\text{ConnTissue}} \\ \nu &= \nu_{\text{Bone}} \cdot \mu_{\text{Bone}} + \nu_{\text{Cartilage}} \cdot \mu_{\text{Cartilage}} + \nu_{\text{ConnTissue}} \cdot \mu_{\text{ConnTissue}} \end{aligned} \quad (5.7)$$

The material properties used in the simulation are presented in Table 5.1 below.

Tissue	Connective tissue	Cartilage	Bone
Young's modulus (MPa)	6 ^a	40 ^b	4000 ^b
Poisson's rate	0.47 ^a	0.35 ^b	0.3 ^b

^a[7]
^b[10]

Table 5.1: Material properties for the tissues.

The mechanical stimulus can be calculated if the material properties and the external load are known. The strain energy density $u(x)$ is used as an indicator for the mechanical stimulus and is given by

$$\begin{aligned}
 u(x) &= \frac{1}{2} \varepsilon^T(x) \cdot \sigma(x) \\
 \varepsilon(x) &= [\varepsilon_x, \varepsilon_y, \varepsilon_z, \gamma_{xy}, \gamma_{yz}, \gamma_{zx}]^T \\
 \sigma(x) &= [\sigma_x, \sigma_y, \sigma_z, \tau_{xy}, \tau_{yz}, \tau_{zx}]^T
 \end{aligned} \tag{5.8}$$

5.3.3 The Fuzzy controller

If the stimulus $u(x)$ and $c(x)$ are known, the tissue reaction can be model. For that purpose a fuzzy controller has been designed. It contains three parts; fuzzyfication, fuzzy rules and defuzzyfication.

5.3.3.1 Fuzzyfication

In order to include the representation of both stimuli $u(x)$ and $c(x)$ in the concept of fuzzy logic, they must be assigned to fuzzy sets. The mechanical stimulus $u(x)$ is classified into four fuzzy sets; low, physiological, increased and pathologic. For the osteogenic factor $c(x)$ the fuzzy sets: poor and high are distinguished. The degrees of membership of these fuzzy sets varies between 0 and 1 continuously, and are defined by membership functions (see [10]) for all values of $u(x)$ and $c(x)$. Subsequently the fuzzy formulation for the mechanical stimulus $u(x)$ is

$$\{\mu_{\text{Low}}, \mu_{\text{Physiological}}, \mu_{\text{Increased}}, \mu_{\text{Pathologic}}\} \tag{5.9}$$

and the fuzzy formulation for the osteogenic factor $c(x)$ is

$$\{\mu_{\text{Poor}}, \mu_{\text{High}}\} \tag{5.10}$$

5.3.3.2 The fuzzy rules

Hofer et al [10] derived a set of fuzzy rules, based on the obtained fuzzy formulations of the stimuli, the tissue composition and medical knowledge. These rules describe tissue transformation, such as intramembranous or endochondral ossification, atrophy or destruction, see Figure 5.4.

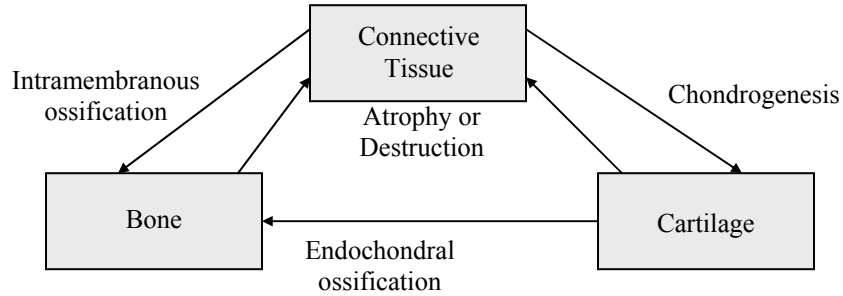


Figure 5.4: Tissue transformation processes.

There are two processes of ossification: intramembranous ossification and endochondral ossification. Furthermore there are two ways of tissue resorption: atrophy and destruction of tissue. Intramembranous ossification needs a high osteogenic factor and a physiological or increased mechanical stimulus. A low mechanical stimulus leads to atrophy of bone or cartilage and a high mechanical stimulus results in destruction of bone or cartilage. The fuzzy rules, R_1 - R_9 are summarized in Table 5.1.

R_1	IF $\mu_{\text{ConnTissue}}$ AND μ_{High} AND $\mu_{\text{Physiologic}}$ THEN intramembranous ossification
R_2	IF $\mu_{\text{ConnTissue}}$ AND μ_{High} AND $\mu_{\text{Increased}}$ THEN intramembranous ossification
R_3	IF $\mu_{\text{Cartilage}}$ AND μ_{High} AND $\mu_{\text{Physiologic}}$ THEN endochondral ossification
R_4	IF $\mu_{\text{Cartilage}}$ AND μ_{High} AND $\mu_{\text{Increased}}$ THEN endochondral ossification
R_5	IF $\mu_{\text{ConnTissue}}$ AND μ_{Poor} AND $\mu_{\text{Increased}}$ THEN chondrogenesis
R_6	IF μ_{Bone} AND μ_{Low} THEN atrophy of bone
R_7	IF $\mu_{\text{Cartilage}}$ AND μ_{Low} THEN atrophy of cartilage
R_8	IF μ_{Bone} AND $\mu_{\text{Pathologic}}$ THEN destruction of bone
R_9	IF $\mu_{\text{Cartilage}}$ AND $\mu_{\text{Pathologic}}$ THEN destruction of cartilage

Table 5.1: The fuzzy rules.

The structure of the fuzzy rules is

IF *premise* THEN *conclusion*

The *premise* has the notation μ_a AND μ_b is replaced by

$$p_{R_n} = \mu_a \mu_b \quad (5.11)$$

Where p_{R_n} is the degree of membership for the premises corresponding to rule R_n and $n = 1 \dots 9$.

5.3.3.3 Defuzzyfication

To achieve the effective tissue transformation rates $d/dt(\mu_{\text{Bone}})$, $d/dt(\mu_{\text{Cartilage}})$ and $d/dt(\mu_{\text{ConnTissue}})$, the rates of Table 5.2 (see [10]) are weighted by the degree of membership for the corresponding premise, and summed up over the whole set of rules. The effective tissue transformation rates $d/dt(\mu_{\text{Bone}})$, $d/dt(\mu_{\text{Cartilage}})$ and $d/dt(\mu_{\text{ConnTissue}})$ are then given by

$$\frac{d}{dt} \mu_t = p_{R_n} \cdot \text{Rate}_{R_n} \quad (5.12)$$

where the subscript t indicates the tissue type, i.e. bone, cartilage or connective tissue, p_{R_n} is the degree of membership for the premises corresponding to rule R_n given by Equation 5.11, and Rate_{R_n} is the tissue transformation rate for rule R_n , which can be found in Table 5.2.

Fuzzy rule, R_n	From (-)	To (+)	Rate R_n (\pm) (%/day)
R_1 and R_2	Connective tissue	Bone	1
R_3 and R_4	Cartilage	Bone	2
R_5	Connective tissue	Cartilage	5
R_6	Bone	Connective tissue	4
R_7	Cartilage	Connective tissue	8
R_8	Bone	Connective tissue	10
R_9	Cartilage	Connective tissue	20

Table 5.2: Tissue transformation rates of the fuzzy rules.

5.3.4 Calculation of a new tissue composition

If the tissue composition in step k is known, the tissue composition in step $(k+1)$ can be calculated as

$$\mu_t^{(k+1)} = \mu_t^{(k)} + \Delta t \frac{d}{dt} \mu_t^{(k)} \quad (5.13)$$

where the subscript t indicates the tissue type, i.e. bone, cartilage or connective tissue, Δt is the time step and $\frac{d}{dt} \mu_t$ is the effective tissue transformation rate given by Equation 5.12.

Chapter 6

Models

At 3 weeks after implantation of the bone chamber in the rat tibia, the tissue within the chamber contains four parts; soft tissue, bone plate, bone and marrow. After studying several samples, a simplified model of the content in a typical chamber was constructed, see Figure 6.1.

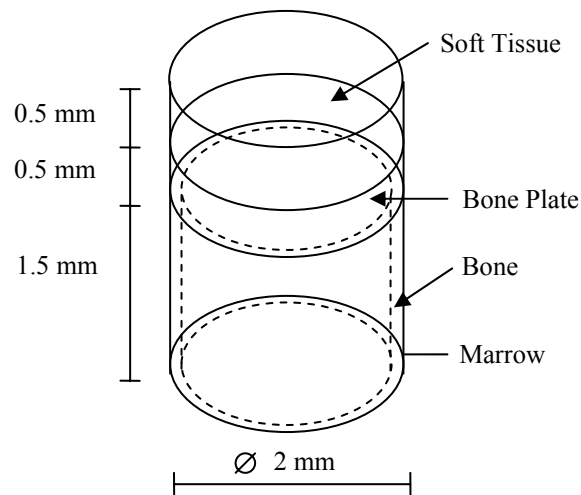


Figure 6.1: The simplified model.

One three-dimensional and one two-dimensional finite element model were implemented in Matlab based on the geometry illustrated in Figure 6.1. The three-dimensional model was used when the hypotheses proposed by Carter et al [7] and Claes et al [9] were tested. To test the fuzzy logic model proposed by Hofer et al [10] the three-dimensional model was redefined into a two-dimensional, see Figure 6.2. The two-dimensional model contains two parts; soft tissue and bone plate. The marrow with surrounding bone is replaced with boundary conditions in the two-dimensional finite element model.

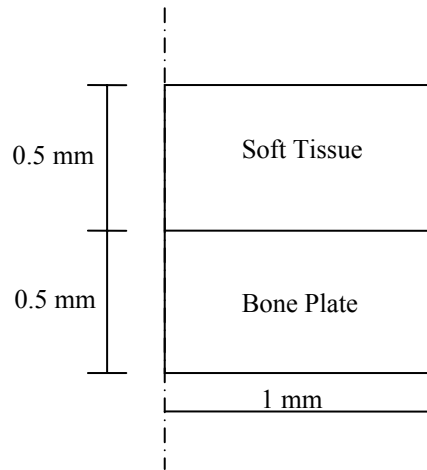


Figure 6.2: The two-dimensional axi-symmetrical geometry.

6.1 The three-dimensional finite element model

Because of the in-growth openings (see Figure 4.2a) there was only one plane of symmetry. To reduce computational cost the only plane of symmetry was used, i.e. the finite element model had a shape of a half cylinder instead of a cylinder. The finite element model consisted of 192 eight-node isoparametric solid elements. Each element contained eight gauss points i.e. two integration points were used when the finite element equations were evaluated. All four types of tissue (see Figure 6.1) were assumed to be linear elastic and isotropic materials. The material properties for the initial state are presented in Table 6.1 below.

Tissue	Soft Tissue	Bone Plate	Bone	Marrow
Young's modulus (MPa)	6 ^a	3000 ^c	5000 ^c	2 ^b
Poisson's ratio	0.47 ^a	0.3 ^c	0.3 ^c	0.25 ^b

^a[7]

^b[11]

^c[Experimental results from the biomechanical laboratory at Lund University Hospital]

Table 6.1: Material properties for the four different tissues.

The finite element mesh of the model is shown in Figure 6.3. The nodes corresponding to the in-growth opening are marked with circles.

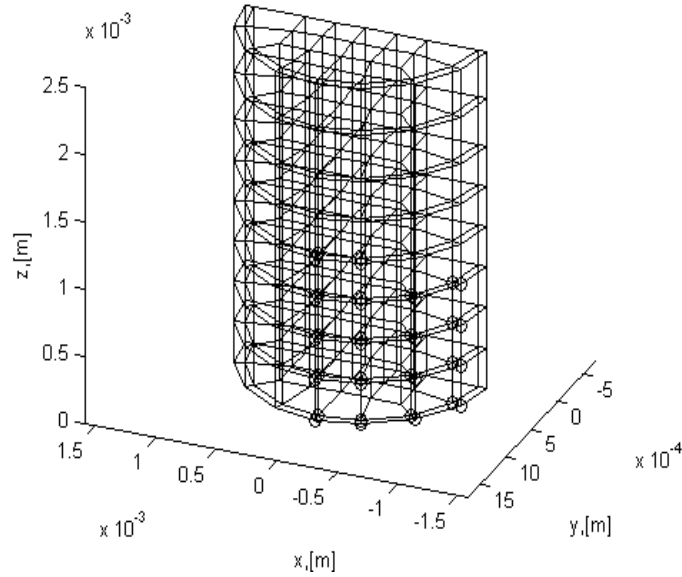


Figure 6.3: Three-dimensional finite element mesh; element nodes marked with circles corresponds to the in-growth opening.

6.1.1 Loading and boundary conditions

At the top surface of the half cylinder a constant pressure of 2 MPa was applied. Friction forces acts on the outer convex surface of the cylinder due to the pressure. The loading situation is illustrated in Figure 6.4.

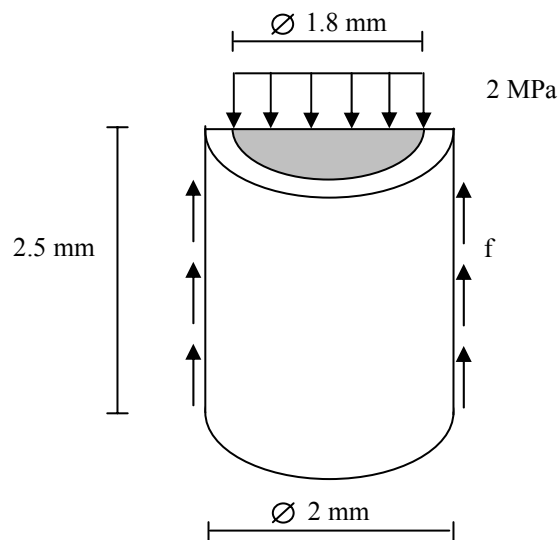


Figure 6.4: The loading situation for the three-dimensional finite element model.

The friction forces were not known from the experiment described in Chapter 4. The following approximate method was used to estimate the friction forces and to avoid the contact problem. The reaction forces acting on the nodes belonging to the outer convex surface (besides from the nodes belonging to the in-growth opening) were calculated when the pressure was applied on the top. From the reaction forces the normal forces were estimated. If the reaction force was a tensile force the corresponding normal force was set to zero. Subsequently the friction forces f were calculated as

$$f = \mu N \quad (6.1)$$

where μ is the friction coefficient between the walls of the chamber and the tissue, and N is the normal force acting on the tissue. The friction coefficients are presented in Table 6.2 below.

Tissue	Bone	Soft Tissue
Friction coefficient (μ)	0.5 ^a	0.15 ^b

^a[12]
^b[13]

Table 6.2: Friction coefficients for bone and soft tissue.

The elements that belonged to the in-growth opening (see Figure 6.3) were not loaded. In the experiment the load of 2 MPa was applied by hand. This means that we have a human source of error. There is also an uncertainty for the values of the friction coefficients between the titanium wall and the soft tissue respectively the bone. Moreover, the material properties for soft tissue and bone are shifting widely in the literature within the biomechanical field. All these mentioned sources of errors may in some sense justify my decision to use an approximate method for estimating the friction forces due to the pressure.

The walls and the bottom of the chamber are assumed to be rigid. With the coordinate system shown in Figure 6.3 the boundary conditions for the displacements were as follows. The displacement degrees of freedom in the x-direction (dof-x) and y-direction (dof-y) of the nodes belonging to the outer convex surface of the cylinder were set to zero except for the nodes that belonged to the in-growth opening. Because of symmetry dof-y of the nodes on the surface coinciding with the symmetry plane were set to zero. Further, dof-z of the nodes situated at the bottom of the cylinder, were also zero.

6.2 The two-dimensional finite element model

A two-dimensional finite element model was implemented in Matlab based on the geometry defined in Figure 6.2. The finite element model consisted of 100 four-node isoparametric solid elements with axi-symmetry. The soft tissue and the bone plate were assumed to be linear elastic and isotropic materials. The initial material properties are presented in Table 6.3.

Tissue	Soft Tissue	Bone Plate
Young's modulus (MPa)	6 ^a	4000 ^b
Poisson's rate	0.47 ^a	0.3 ^b

^a[7]
^b[10]

Table 6.3: Material properties for the initial state.

The finite element mesh of the two-dimensional axi-symmetrical model is shown in Figure 6.5.

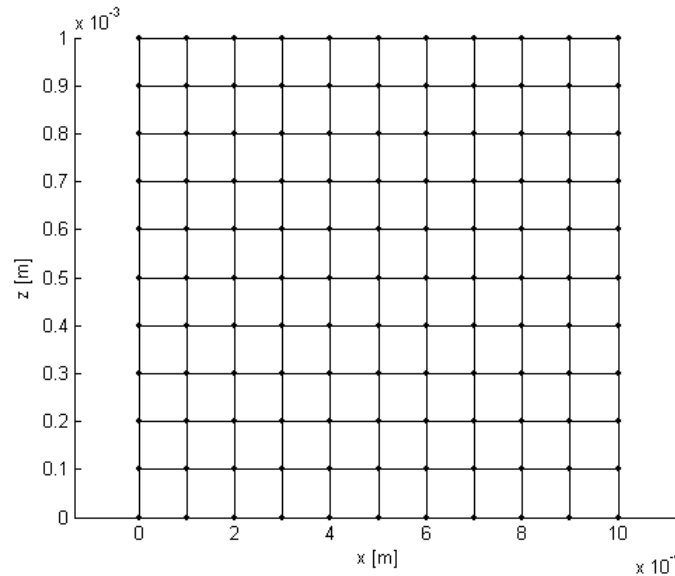


Figure 6.5: The two-dimensional finite element mesh.

6.2.1 Loading and boundary conditions

A pressure of 2 MPa is applied on the top of the model. Due to the pressure friction forces acts on the contact surface between the walls of the chamber and the tissue, see Figure 6.6. The friction forces f , were calculated with the method introduced in Chapter 6.1.1. In the fuzzy logic model the tissue formation is simulated during time. This means that it is possible that the material properties of the elements on the side surface where the friction forces are acting changes during time. To simplify the calculations the material properties on the side surface where the friction forces are acting were assumed to be unchanged, i.e. the friction coefficient for soft tissue and bone are used and the friction coefficient for cartilage is not introduced. The loading situation and the boundary conditions for the two-dimensional model are presented in Figure 6.6.

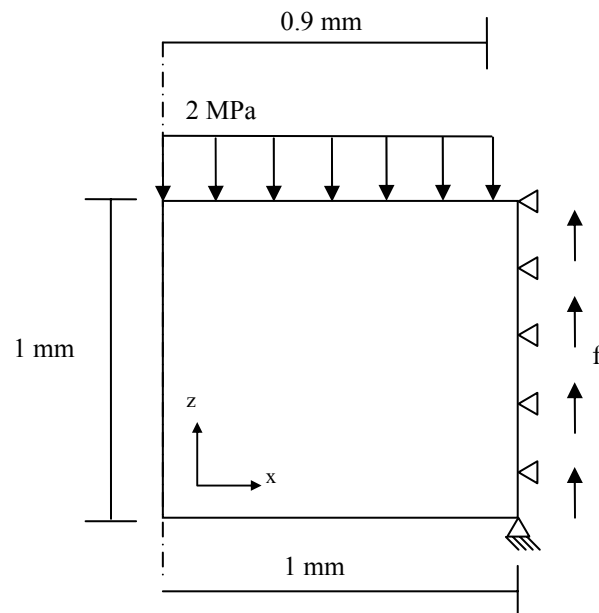


Figure 6.6: The loading situation and the boundary conditions for the two-dimensional axi-symmetrical model.

Chapter 7

Results

In this chapter the results from the finite element analyses, with the methods and models described in chapter 5 and 6, are presented.

7.1 Carters hypothesis

A finite element analysis was performed with the three-dimensional model presented in Chapter 6.1. The slope and position of the straight line in Figure 5.1a, which divides the region of bone from the region of cartilage, was first identified. According to the experiment, cartilage was found in the chamber beneath the piston, after 7 weeks of loading. The region, where cartilage was found in the experiment, corresponds to the top of the finite element model. The octahedral shear stress and dilatational stress were calculated for the gauss points in each of the elements within the intervals $1.5 \leq z \leq 1.8$ mm and $2.2 \leq z \leq 2.5$ mm, i.e. the elements belonging to the bone plate respectively the soft tissue on the top of the model, see Figure 6.1. The octahedral shear stresses were then plotted versus the dilatational stresses, see Figure 7.1 below.

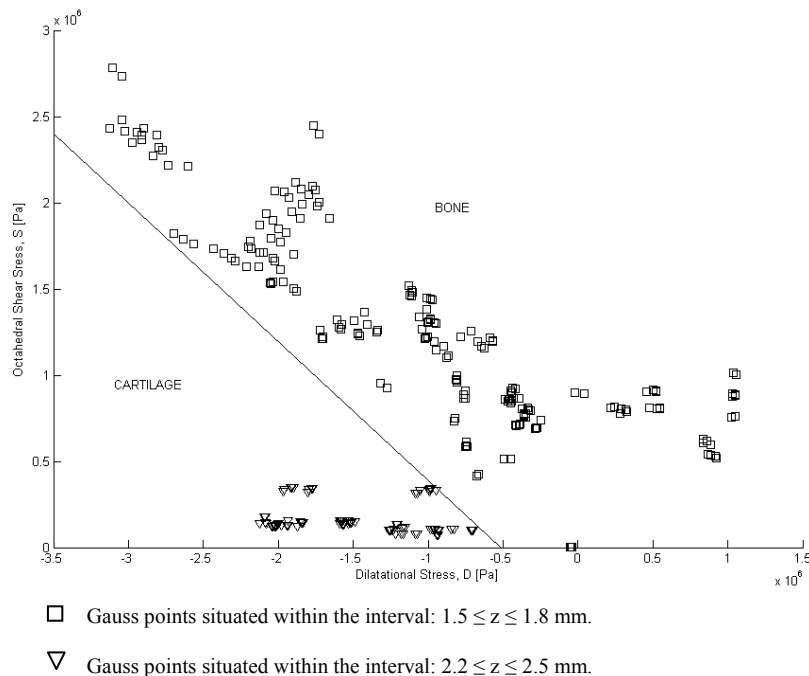


Figure 7.1: Octahedral and dilatational stresses within the intervals; $1.5 \leq z \leq 1.8$ mm and $2.2 \leq z \leq 2.5$ mm .

The squares in Figure 7.1 correspond to gauss points initially belonging to the bone plate. The triangles correspond to the gauss points on the top. It appeared that the values of the gauss points on the top were gathered together in one region, and the values of the gauss points corresponding to the bone plate, in another. Subsequently, the slope and position of a straight line which separate the both regions from each other was approximately estimated, see Figure 7.1. The slope of the line was determined to -0.8 and the value of the dilatational stress where the line intersects with the D-axis was determined to -0.5 MPa. The reference value of the osteogenic index was then calculated to be -0.4 MPa using Equation 5.2, where $k = 0.8$, $D = -0.5$ MPa and $S = 0$.

The reference value serves as a threshold value for determining whether bone or cartilage will form. If the osteogenic index fulfills the condition $I < -0.4$ MPa, cartilage is predicted, whereas if $I > -0.4$ MPa bone will form.

The osteogenic index I was then calculated for the elements within the interval $1.5 \leq z \leq 2.5$ mm. Plots of the osteogenic index are presented in Figure 7.2 and 7.3. The area marked with dots ($0 \leq z < 1.5$ mm) corresponds to the marrow with surrounding bone. Since marrow is not represented in Carters hypothesis, the osteogenic index I has not been calculated in this area.

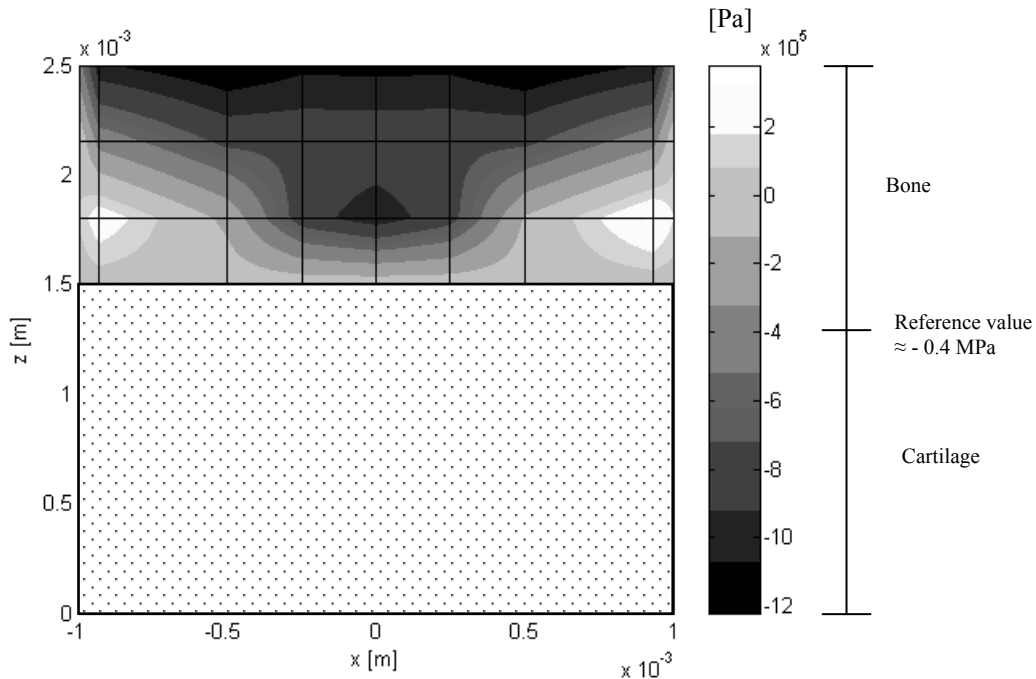


Figure 7.2: Plot of the osteogenic index in the symmetry plane, i.e. the y-coordinates are zero.

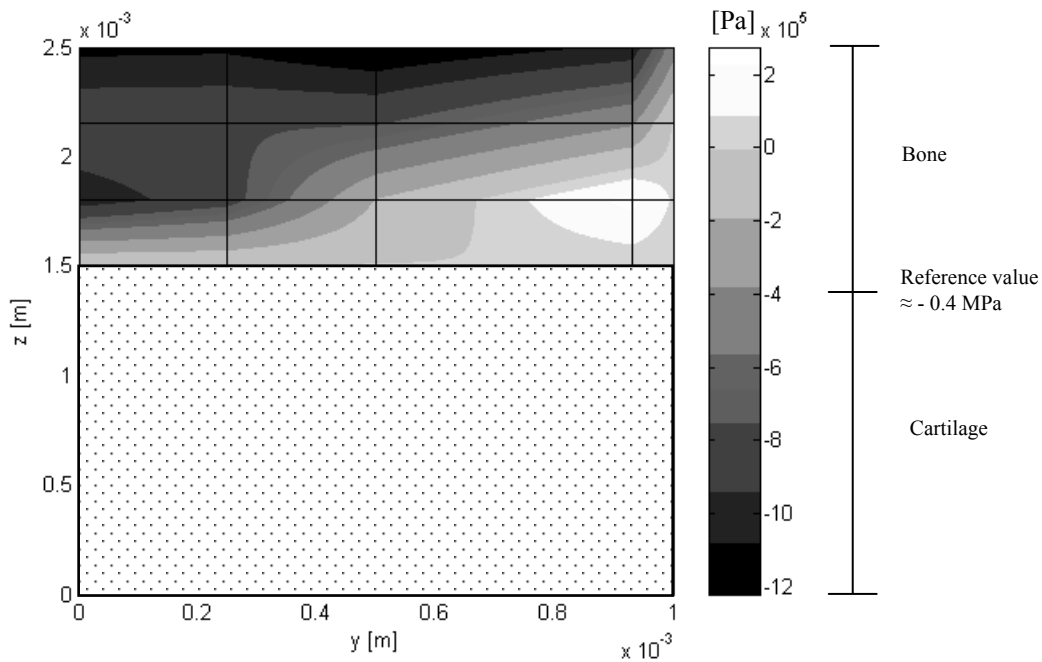


Figure 7.3: Plot of the osteogenic index in the yz-plane.

A region of cartilage is predicted on the top the model i.e. $2.2 \leq z \leq 2.5$ mm, followed by a region of bone; $1.5 \leq z < 2.2$ mm. In the middle of the identified region of bone ($z \approx 1.8$ mm) there are some gauss points which are predicted to be cartilage. Above these gauss points there is a layer of bone. This phenomenon is not clear from the plots of the osteogenic index. A more comprehensive illustration of this phenomenon is achieved with a plot in the SD-plane, see Figure 7.4 below.

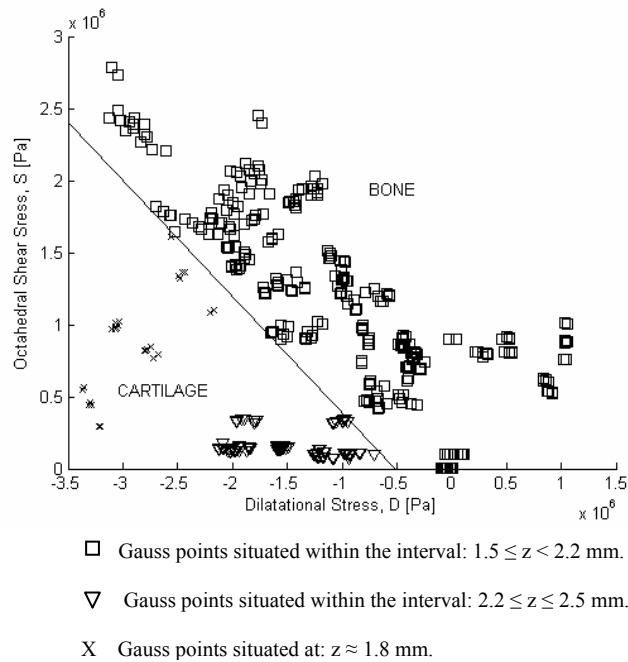


Figure 7.4: Values of the octahedral and dilatational stress for the gauss points within the interval; $1.5 \leq z \leq 2.5$ mm .

The x-marks in Figure 7.4 represent the gauss points which were detected in the middle of the identified bone region but were predicted to be cartilage i.e. the gauss points situated at $z \approx 1.8$ mm. The squares represent the gauss points of the identified bone region ($1.5 \leq z < 2.2$ mm), whereas the triangles represent the gauss points of the identified cartilage region on the top ($2.2 \leq z \leq 2.5$ mm).

7.2 Claes hypothesis

A finite element analysis was performed with the three-dimensional model described in Chapter 6.1. The strain in the loading direction (see Figure 6.4) and dilatational stresses (hydrostatic pressure) were calculated for the gauss points in each element within the interval $1.5 \leq z \leq 2.5$ mm and plotted versus each other. The results can be seen in Figures 7.5-7.7. In the regions denoted by A and B, bone respectively cartilage is predicted. Connective tissue/fibrocartilage is indicated in the region termed C. This is in agreement with the graphical interpretation of Claes hypothesis presented in Chapter 5.

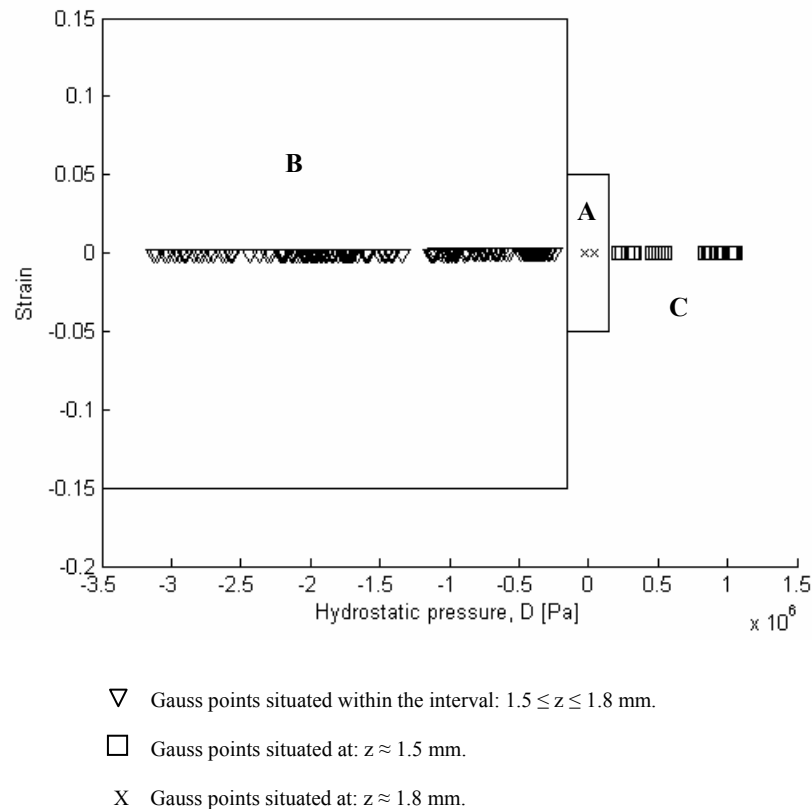


Figure 7.5: Strain and hydrostatic pressure of the gauss points initially belonging to the bone plate; $1.5 \leq z \leq 1.8$ mm.

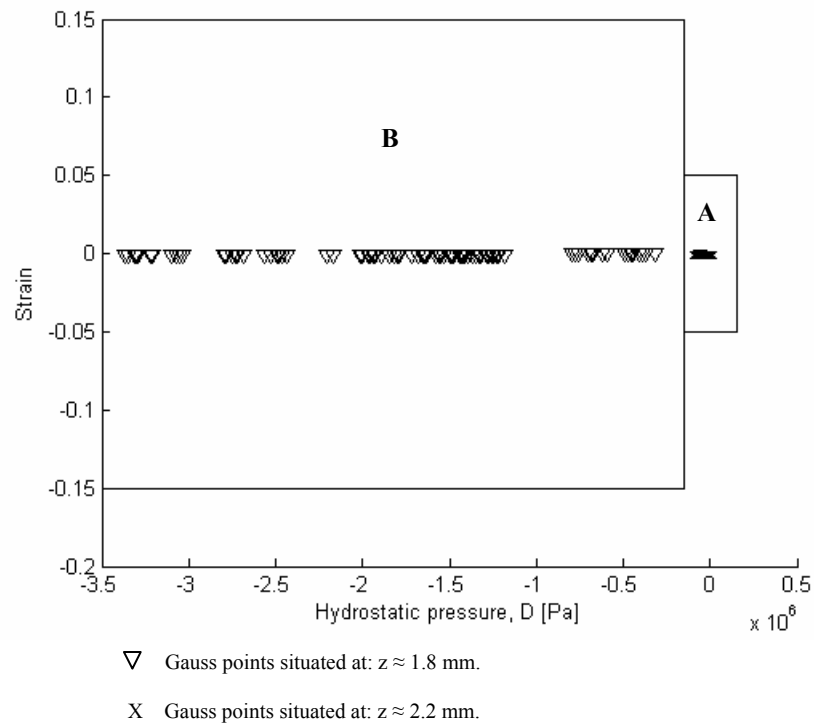


Figure 7.6: Strain and hydrostatic pressure of the gauss points initially belonging to soft tissue (connective tissue); $1.8 < z \leq 2.2$ mm .

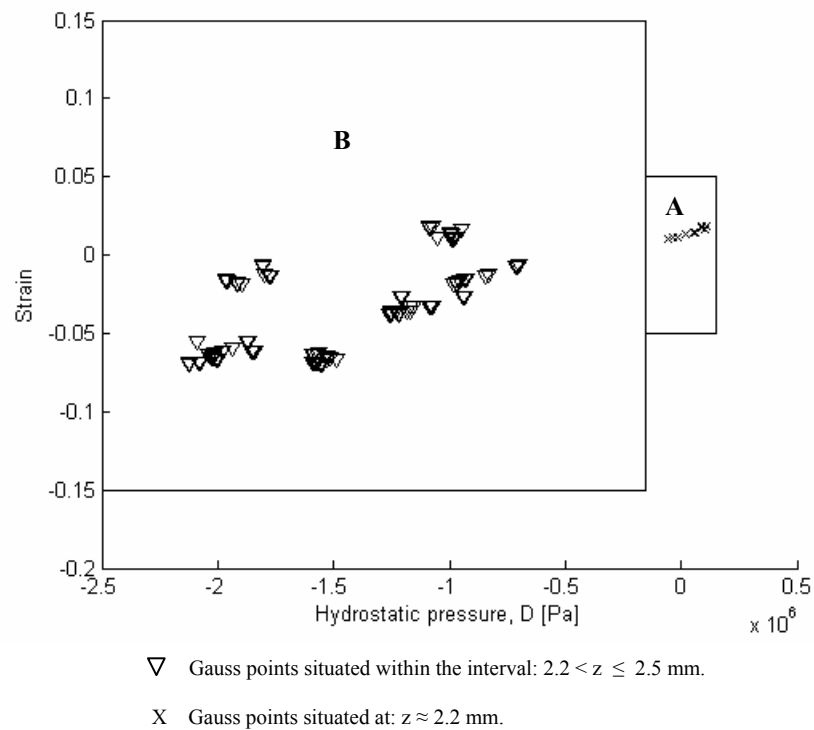


Figure 7.7: Strain and hydrostatic pressure of the gauss points initially belonging to soft tissue (connective tissue); $2.2 < z \leq 2.5$ mm .

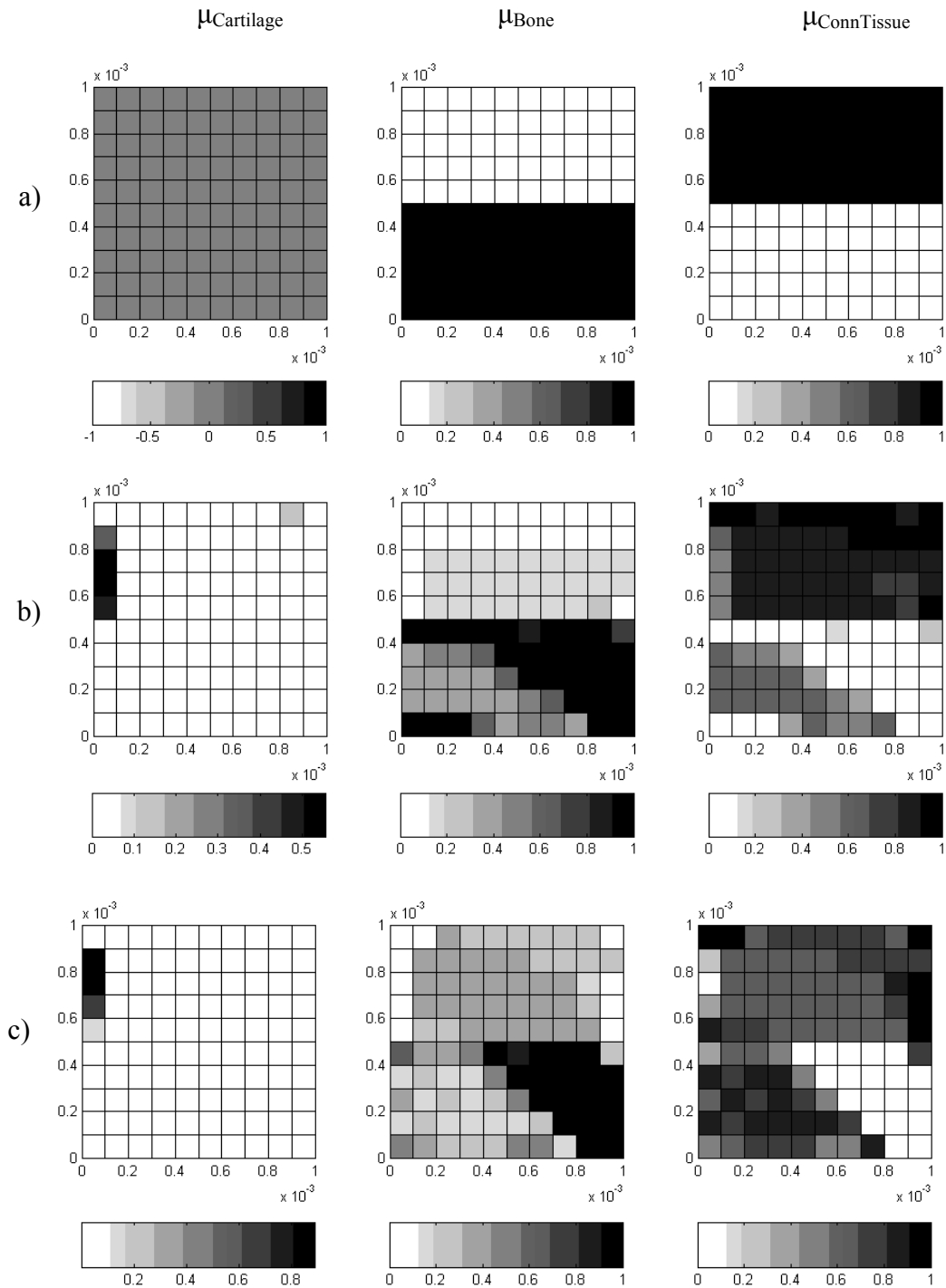
The majority of the gauss points that initially belonged to the bone plate are predicted to be cartilage or connective tissue/fibrocartilage, see Figure 7.5. Only two of the gauss points are predicted to be bone. Above this identified region of cartilage, a layer of bone is indicated at $z \approx 2.2$ mm. On the top of the model, i.e. $2.2 \leq z \leq 2.5$ mm, an additional region of cartilage is predicted.

7.3 Fuzzy logic model by Hofer

To simulate the course of events during the 7 weeks, when the tissue inside the bone chamber was loaded, a model proposed by Hofer et al [10] was used. The calculations were executed with the procedure described in Chapter 5.3 and the finite element model described in Chapter 6.2. The results from the simulation after 3 and 7 weeks of loading are presented in Figure 7.8. At the initial state there is only soft tissue (connective tissue) and bone, i.e. the degree of membership for cartilage is equal to zero for each element, see Figure 7.8a.

After 3 weeks of loading, a small amount of soft tissue has been transformed into cartilage in the middle of the region, which initially consisted of connective tissue, see Figure 7.8b. Furthermore, connective tissue is found in elements situated at the centre of the region, which initially represented the bone plate. Some of the elements has almost completely transformed from bone to connective tissue i.e. the degree of membership for connective tissue is nearly 1, whereas some of the elements only consists of a very small amount of connective tissue.

After 7 weeks there is an indication of cartilage in the middle, on the top of the model. However none of the elements, which contain cartilage, have a degree of membership for cartilage which is equally to 1. The region of connective tissue that was detected after 3 weeks is further extended and there are some elements which now completely have been transformed into connective tissue.



z [m]
 \uparrow
 x [m]

Figure 7.8: The degree of membership μ for cartilage, bone and connective tissue:

- a) At the initial state
- b) After 3 weeks of loading
- c) After 7 weeks of loading

In Figure 7.9 the change of degree of membership for cartilage and connective tissue (soft tissue) for element number 21, during 7 weeks of loading with a pressure of 2 MPa, can be seen. This element is situated in the middle on the top of the model. As a consequence of the applied load, the degree of membership for cartilage is increasing with time, whereas the degree of membership for connective tissue is decreasing. The degree of membership for bone of the element is equal to zero at the initial state and does not change during the time of loading.

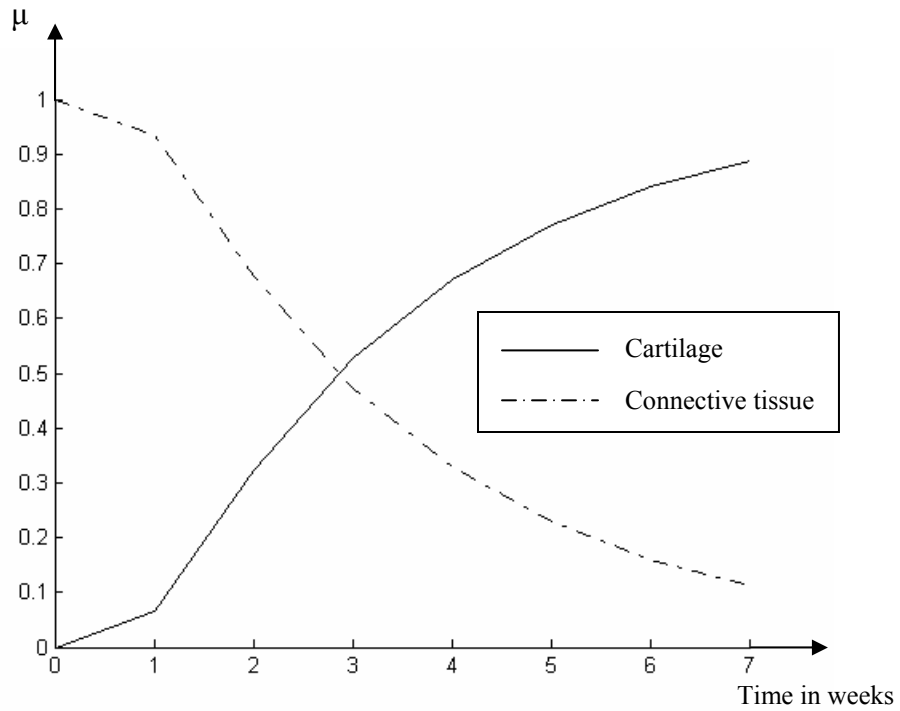


Figure 7.9: The change of degree of membership for cartilage and connective tissue for element number 21 during 7 weeks of loading with a pressure of 2 MPa.

Chapter 8

Discussion and future work

The result from the finite element analysis with Carters hypothesis is similar to the result from the experiment, in which cartilage was found on the top after loading followed by a region of bone. The result from the analysis with Claes hypothesis does not correlate so well with the experiment. After loading, cartilage is indicated on the top of the model and followed by a region of bone. This is in analogy with the results from the experiment. However there is a layer of cartilage predicted beneath the region of bone, which not has been observed in the experiment.

According to the analysis with Hofers model, cartilage will form in the middle, on the top of the model after 7 weeks of loading. However the predicted area of cartilage is very small in comparison with the results from the finite element analyses when Carter and Claes hypothesis were used. Further, a part of the bone plate has been transformed into connective tissue. This means that the elements belonging to this part of the bone plate has undergone a process of atrophy or destruction, see Figure 5.4. A low mechanical stimulus leads to atrophy of bone and a high mechanical stimulus results in destruction of bone. After studying some of the elements belonging to the region it turned out that there are some elements that undergo the process of atrophy and others that experience the process of destruction. Consequently the region experiences both high and low mechanical stimuli.

The material properties of the tissues are shifting widely in the literature within the biomechanical field. This means that the results from the finite element analyses must be handled with care. In a future experiment with the bone chamber different values of applied load at the top are suggested, to get a better verification of the results from the finite element analyses. Further, the bone chamber should be harvested at several different points of time, which is needed to get more detailed information of the course of events during the time of loading. Finite element analyses have been performed with the model proposed by Hofer with different values of the pressure. According to these analyses a value below 2 MPa is recommended in future experiments.

It shall be emphasized that the fuzzy rules are based on the study made by Hofer et al [10]. It is very likely that these set of rules are not ideal for the study Tägil et al [2] made. One specific improvement that could be made in Hofers model is therefore a new set of fuzzy rules. Further, in future models it is suggested that the effect of the fluid flow acting within the tissue is considered, i.e. poro elastic models are recommended.

References

- [1] Sean Hughes, Ian McCarthy, 1998. Science Basic to Orthopaedics. WB Saunders Company Limited.
- [2] Magnus Tägil, Per Aspenberg, 1999. Cartilage induction by controlled mechanical stimulation in vivo. *Journal of Orthopaedic Research* 17:200-204.
- [3] S.C. Cowin, 1981. Introduction to the symposium on the mechanical properties of bone. *Mechanical properties of bone*. ASME, AMD-Vol.45.
- [4] B.Sonesson, G.Sonesson. *Människans anatomi och fysiologi*, 1993, Liber.
- [5] B.M.Nigg, W.Herzog. *Biomechanics of the musculo-skeletal system-second edition*, 1999. John Wiley & Sons.
- [6] A.Bailón-Plaza, C.H.Van Der Meulen, 2001. A mathematical framework to study the effects of growth factor influences on fracture healing. *J.theor.Biol.*, 212,191-209.
- [7] D.R.Carter, P.R. Blenman, G.S.Beaupré, 1988. Correlations between mechanical stress history and tissue differentiation in initial fracture healing. *Journal of Orthopaedic Research*, 6:736-748.
- [8] N.S Ottosen and M. Ristinmma. *The mechanics of constitutive modeling*, volume 1. Division of Solid Mechanics, Lund 1999.
- [9] L.E Claes, C.A Heigele, 1998. Magnitudes of local stress and strain along bone surfaces predict the course and type of fracture healing. *Journal of biomechanics* 32 (1999) 255-266.
- [10] Ch.Ament, E.P.Hofer, 2000. A fuzzy logic model of fracture healing. *Journal of biomechanics* ,33 (2000) 961-968.
- [11] D.Lacroix, P.J.Prendergast, 2002. A mechano-regulation model for tissue differentiation during fracture healing: analysis of gap size loading. *Journal of Biomechanics* 35:1163-1171.
- [12] A.Shirazi-Adl, M.Dammak, G.Paiement, 1993. Experimental determination of friction characteristics at the trabecular bone/porous-coated metal interface in cementless implants. *Journal of Biomedical Materials Research*, 27:167-175.
- [13] P.A. Lilley, M.Raine, G.W.Blunn, 1998. Simulation of the wear of metal implants by soft-tissue. *International Conference on Simulation*, 30 September-2 October 1998, Conference Publication No.457.

Appendix A

Some medical expressions often used in the thesis

Apposition: Growth in the thickness of a cell wall by the deposit of successive layers of material.

Callus: Tissue which forms round a broken bone as it starts to mend, leading to consolidation.

Embryonic: In an early stage of development.

Diaphyseal: Referring to diaphysis.

Diaphysis: Shaft or long central part of a long bone.

Endosteal: Referring to the endosteum.

Endosteum: Membrane lining the bone marrow cavity inside a long bone.

Fibrin: Protein produced by fibrinogen, which helps make blood coagulates.

Haematoma: Mass of blood under the skin caused by a blow or by the effects of an operation.

Histology: Study of anatomy of tissue cells and minute cellular structure, done using a microscope after the cells have been stained.

In vivo: Experiment which takes place on the living body.

Larynx: Organ in the throat which produce sounds.

Medullary: Similar to marrow.

Metatarsal: One of the five long bones in the foot between the toes and the tarsus.

Osteotomy: Surgical operation to cut a bone, especially to relieve pain in a joint.

Perichondrium: Fibrous connective tissue which covers cartilage.

Periosteal: Referring to the periosteum.

Periosteum: Dense layer of connective tissue around a bone.

Paltelet: Little blood cell which encourages the coagulation of blood.

Tarsus: The seven small bones of the ankle.

Appendix B

Criterion by Drucker-Prager

In the plasticity theory there are different forms of hypotheses which tell us whether plastic deformations (i.e. yielding of the material) or failure occurs. For materials like concrete, soils and rocks, a criterion proposed by Drucker and Prager [8] can be used. The criterion is given by

$$\sqrt{3J_2} + \alpha I_1 - \beta = 0 \quad B.1$$

where α and β are material parameters and J_2 and I_1 are stress invariants. In Figure B.1 the Drucker-Prager criterion is presented in the meridian plane.

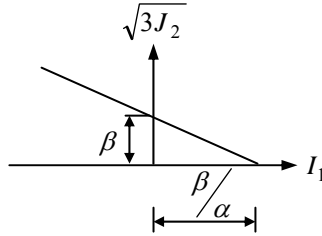


Figure B.1: The Drucker-Prager criterion illustrated in the meridian plane.

A physical interpretation of the Drucker-Prager criterion is that failure or yielding occurs when the octahedral shear stress exceeds a certain value that depends on the octahedral normal stress.

The osteogenic index I that was introduced in Carters hypothesis [7] is given by Equation 5.2. If the octahedral shear and dilatational stress are expressed in terms of stress invariants Equation 5.2 read as

$$I = \sqrt{\frac{2}{3}J_2} + k \cdot \frac{1}{3}I_1 \quad B.2$$

which also can be written on the form

$$\sqrt{\frac{2}{3}J_2} + k \cdot \frac{1}{3}I_1 - I = 0 \quad B.3$$

A comparison between Equation B.1 and B.3 shows that there is an analogy between the initial yield criteria proposed by Drucker and Prager [8] and the hypotheses of tissue differentiation proposed by Carter et al [7].

Appendix C

In this appendix the Matlab codes used in the thesis are presented. The geometry files of both of the finite element models have been excluded since they are too sparse to print. For the same reason, the Matlab files calculating the boundary conditions and the total loading situation of the three-dimensional model have been excluded.

Matlab Code

Hypotheses by Carter and Claes

```
% -----Main program Carter/Claes part1 -----%

load C:\kmatris K D
% --- f1 corresponds to the load vector acting at the top of the model ----
load C:\fload1 f1
load C:\bc bc

% --- Calculation of the displacements a and reaction forces Q ---
[a,Q]=solveq(K,f1,bc);

The reaction forces Q → the friction forces acting at the outer surface → calculation of f2 ---
save C:\Qforce Q

% -----End -----%

% -----Main program Carter/Claes part2 -----%

load C:\Geom
load C:\kmatris K D
load C:\bc bc

% --- f2 = the total force vector = f1 + friction forces ---
load C:\fload_2 f2

a=solveq(K,f2,bc);
Ed=extract(Edof,a);

% --- One row for each gauss point ---
Es=zeros(8*nel,6);
Et=zeros(8*nel,6);
Etz=[];
ep=[2];
Dcount=1;
r=1;

for i=1:nel
    [es,et]=soli8s_mod(Ex(i,:),Ey(i,:),Ez(i,:),ep,D(Dcount:(Dcount+5),:),Ed(i,:));
```

```

        Es(r:r+7,:)=es;
        Et(r:r+7,:)=et;
        Etz(i,:)=et(1:8,3)';
        r=r+8;
        Dcount=Dcount+6;
end
load C:\tissue_1

[Soct,Doct]=carter_1(Es,nel);

save C:\octstress_1 Soct Doct
save C:\strain_z E_tz

% -----End -----%

%-----Calculation of the initial tissue vector -----%

%      tissue=[elnum k k k k k k k my] one value of k for each gauss point → 8 k-values
%      k=1,2,3,4
%      1=Soft tissue (connective tissue)
%      2=Bone
%      3=Bone plate
%      4=Marrow
% -----

tissue=[ ];
load C:\Geom
mybone=0.3;
mysoft=0.15;

for i=1:(24+4*24)
    switch i
        case {1,1+24,1+2*24,1+3*24,1+4*24,9,9+24,9+2*24,9+3*24,9+4*24,21,21+24,21+2*24,21+3*24,
                21+4*24,22,22+24,22+2*24,22+3*24,22+4*24,23,23+24,23+2*24,23+3*24,23+4*24,
                24,24+24,24+2*24,24+3*24,24+4*24,16,16+24,16+2*24,16+3*24,16+4*24,
                8,8+24,8+2*24,8+3*24,8+4*24}

            % --- local gauss point 1,4,5,8 = Bone ---
            tissue(i,2)=2;
            tissue(i,5)=2;
            tissue(i,6)=2;
            tissue(i,9)=2;

            % --- local gauss point 2,3,6,7 = Marrow---
            tissue(i,3:4)=4;
            tissue(i,7:8)=4;
            tissue(i,1)=i;

            % --- friction coefficient at the outer surface---
            tissue(i,10)=mybone;

        otherwise
            %---marrow
            tissue(i,2:9)=4;
            tissue(i,1)=i;
    end
end

```

```

        tissue(i,10)=0;    % --- Marrow does not exist at the outer surface---
    end
end

for i=(1+5*24):(24+5*24)

    % --- Bone plate---
    tissue(i,2:9)=3;
    tissue(i,1)=i;
    % --- friction coefficient at the outer surface ---
    tissue(i,10)=mybone;
end

for i=145:168

    for j=2:9

        % --- local gauss point 1,2,3,4 = bone ---
        if j==2
            tissue(i,j)=3;
        elseif j==3
            tissue(i,j)=3;
        elseif j==4
            tissue(i,j)=3;
        elseif j==5
            tissue(i,j)=3;
        else
            % --- local gauss point 5,6,7,8 = soft tissue (connective tissue) ----
            tissue(i,j)=1;
        end
    end

    tissue(i,1)=i;
    % --- friction coefficient at the outer surface ---
    tissue(i,10)=mybone;

end

for i=169:nel

    % --- Soft tissue (connective tissue) ---
    tissue(i,2:9)=1;
    tissue(i,1)=i;
    % --- friction coefficient at the outer surface ---
    tissue(i,10)=mysoft;
end

save C:\tissue_1 tissue

% -----End-----%

```

```

%----Calculation of the constitutive matrix D and the global stiffness matrix K-----%

clear all;
load C:\Geom

% --- number of gauss points=2 --> 8 gauss points in each element ---
ep=[2]; K=zeros(ndof); Ke=zeros(24);
D=[ ]; De=[ ]; Dgp=[ ];
load C:\tissue_1 tissue

%-----
%      tissue=[elnum k k k k k k k k my], one value of k for each gauss point --> 8 k-values
%      k=1,2,3,4
%      1=soft tissue(connective tissue)
%      2=bone
%      3=boneplate
%      4=marrow
%-----
Dcount=1;

for elnum=1:nel
    r=1;
    for i=2:9
        k=tissue(elnum,i);
        switch k
            case{1}
                % --- Constitutive matrix soft tissue (connective tissue) ---
                E=6e6; v=0.47; Dgp=hooke(4,E,v);
            case{2}
                % --- Constitutive matrix bone ---
                E=5000e6; v=0.3; Dgp=hooke(4,E,v);
            case{3}
                % --- Constitutive matrix bone plate ---
                E=3000e6; v=0.3; Dgp=hooke(4,E,v);
            case{4}
                % --- Constitutive matrix marrow ---
                E=2e6; v=0.25; Dgp=hooke(4,E,v);
        end

        De(:,r:r+5)=Dgp; Dgp=[ ];
        r=r+6;
        % --- De=[Dgp1 Dgp2 Dgp3 Dgp4 Dgp5 Dgp6 Dgp7 Dgp8]---
        %      where Dgpn=constitutive matrix of gauss point number n ---
    end
    D(Dcount:(Dcount+5),:)=De;
    Dcount=Dcount+6;
    Ke=soli8e_mod(Ex(elnum,:),Ey(elnum,:),Ez(elnum,:),ep,De');
    K=assem(E dof(elnum,:),K,Ke);
    Ke=zeros(24);
    De=[ ];
end

save C:\kmatris K D

%-----End-----%

```

%-----Calculation of the load vector fl on the top-----%

```
clear all;
load C:\Geom
f1=zeros(ndof,1);
fe=zeros(24,1);

for i=1:nel
    switch i
        % --- elements on the top ---
        case {2+7*24,3+7*24,4+7*24,5+7*24,6+7*24,7+7*24,10+7*24,11+7*24,12+7*24,13+7*24,
              14+7*24,15+7*24,17+7*24,18+7*24,19+7*24,20+7*24}
            fe=boundary1(Ex(i,:),Ey(i,:));

            otherwise
                fe=zeros(24,1);
            end

            % --- fl corresponds to the load applied at the top ---
            f1=assem_fe(Edof(i,:),f1,fe);
            fe=zeros(24,1);
        end
    end
end
save C:\fload1 f1
```

%-----End-----%

%-----Calculation of the boundary integral on the top with gauss integration -----%

```
function [fe1]=boundary1(ex,ey)

sigmazz=-2e6; %---[Pa]-----

% --- position of the gauss points ---
eta1=1/(sqrt(3));
eta2=-1/(sqrt(3));
ksi1=eta1;
ksi2=eta2;

eta=eta1;
ksi=ksi1;
a1=0.25*[(-1+eta)*ex(1,5)+(1-eta)*ex(1,6)+(1+eta)*ex(1,7)+(-1-eta)*ex(1,8)
         (-1+eta)*ey(1,5)+(1-eta)*ey(1,6)+(1+eta)*ey(1,7)+(-1-eta)*ey(1,8)
         0];
b1=0.25*[(-1+ksi)*ex(1,5)+(-1-ksi)*ex(1,6)+(1+ksi)*ex(1,7)+(1-ksi)*ex(1,8)
         (-1+ksi)*ey(1,5)+(-1-ksi)*ey(1,6)+(1+ksi)*ey(1,7)+(1-ksi)*ey(1,8)
         0];

% ---Nmod=[N5 N6 N7 N8]T when dzeta=0 and zeta=1 → N1=N2=N3=N4=0 ---
Nmod=[0.25*(1-ksi)*(1-eta); 0.25*(1+ksi)*(1-eta); 0.25*(1+ksi)*(1+eta);0.25*(1-ksi)*(1+eta)];
I1=norm(cross(a1,b1))*sigmazz*Nmod;

eta=eta1;
ksi=ksi2;
```

```

a1=0.25*[(-1+eta)*ex(1,5)+(1-eta)*ex(1,6)+(1+eta)*ex(1,7)+(-1-eta)*ex(1,8)
(-1+eta)*ey(1,5)+(1-eta)*ey(1,6)+(1+eta)*ey(1,7)+(-1-eta)*ey(1,8)
0];
b1=0.25*[(-1+ksi)*ex(1,5)+(-1-ksi)*ex(1,6)+(1+ksi)*ex(1,7)+(1-ksi)*ex(1,8)
(-1+ksi)*ey(1,5)+(-1-ksi)*ey(1,6)+(1+ksi)*ey(1,7)+(1-ksi)*ey(1,8)
0];

Nmod=[0.25*(1-ksi)*(1-eta); 0.25*(1+ksi)*(1-eta); 0.25*(1+ksi)*(1+eta);0.25*(1-ksi)*(1+eta)];
I2=norm(cross(a1,b1))*sigmaz* Nmod;
eta=eta2;
ksi=ksi1;
a1=0.25*[(-1+eta)*ex(1,5)+(1-eta)*ex(1,6)+(1+eta)*ex(1,7)+(-1-eta)*ex(1,8)
(-1+eta)*ey(1,5)+(1-eta)*ey(1,6)+(1+eta)*ey(1,7)+(-1-eta)*ey(1,8)
0];
b1=0.25*[(-1+ksi)*ex(1,5)+(-1-ksi)*ex(1,6)+(1+ksi)*ex(1,7)+(1-ksi)*ex(1,8)
(-1+ksi)*ey(1,5)+(-1-ksi)*ey(1,6)+(1+ksi)*ey(1,7)+(1-ksi)*ey(1,8)
0];

Nmod=[0.25*(1-ksi)*(1-eta); 0.25*(1+ksi)*(1-eta); 0.25*(1+ksi)*(1+eta);0.25*(1-ksi)*(1+eta)];
I3=norm(cross(a1,b1))*sigmaz* Nmod;

eta=eta2;
ksi=ksi2;
a1=0.25*[(-1+eta)*ex(1,5)+(1-eta)*ex(1,6)+(1+eta)*ex(1,7)+(-1-eta)*ex(1,8)
(-1+eta)*ey(1,5)+(1-eta)*ey(1,6)+(1+eta)*ey(1,7)+(-1-eta)*ey(1,8)
0];
b1=0.25*[(-1+ksi)*ex(1,5)+(-1-ksi)*ex(1,6)+(1+ksi)*ex(1,7)+(1-ksi)*ex(1,8)
(-1+ksi)*ey(1,5)+(-1-ksi)*ey(1,6)+(1+ksi)*ey(1,7)+(1-ksi)*ey(1,8)
0];

Nmod=[0.25*(1-ksi)*(1-eta); 0.25*(1+ksi)*(1-eta); 0.25*(1+ksi)*(1+eta);0.25*(1-ksi)*(1+eta)];
I4=norm(cross(a1,b1))*sigmaz* Nmod;

I=I1+I2+I3+I4;

fe1=[0 0 0 0 0 0 0 0 0 0 0 0 0 0 0 0 I(1) 0 0 I(2) 0 0 I(3) 0 0 I(4)];

%-----End-----%

%-----Calculation of the octahedral shear stresses Soct, and the dilatational stresses D -----%

function [Soct,Doct]=carter_1(Es,nel)

E=eye(3);

% --- One row for each element, one column for each gauss point ---
D=zeros(nel,8);
es=zeros(8,6);
r=1;

for i=1:nel

    es=Es(r:r+7,:);

    for j=1:8
        s11=es(j,1); s22=es(j,2); s33=es(j,3); s12=es(j,4); s13=es(j,5); s23=es(j,6);

```

```

    sigmatensor=[s11 s12 s13
                s12 s22 s23
                s13 s23 s33];

    L=eigen(sigmatensor,E);
    L=sort(L);
    % --- L(1)=sigma3 L(2)=sigma2 L(3)=sigma1, sigma1>sigma2>sigma3 ---

    Soct(i,j)=(1/3)*sqrt((L(3)-L(2))^2+(L(2)-L(1))^2+(L(1)-L(3))^2);
    Doct(i,j)=(1/3)*(L(3)+L(2)+L(1));

end
    r=r+8;
    es=zeros(8,6);
end

%-----End-----%

```

Fuzzy logic model by Hofer

```

%-----Main program Hofer-----%

clear all;

load C:\Geom_fuzzy
% --- loading the initial state of the degree of membership for bone, cartilage and connective tissue ---
load C:\initial_my_fuzzy myb myc myt

% --- nstep = number of time steps ---
nstep=7*7;

for step=1:nstep
    % ---myb--> osteogenicfactor c [%/mm] ---
    [c]=osteogenic_factor(Ex,Ey,nel,myb);

    K=zeros(ndof);

    for i=1:nel
        % ---mixture rule ---
        E=4000e6*myb(i)+40e6*myc(i)+6e6*myt(i);
        v=0.3*myb(i)+0.35*myc(i)+0.47*myt(i);
        De=hooke(2,E,v);
        Ke=plani4eaxi(Ex(i,:),Ey(i,:),[3 1 1],De);
        K=assem(Edof(i,:),K,Ke);
    end
    % --- Loading the force vector f acting at the top of the model and the boundary vector bc ---
    load C:\load_bc_fuzzy f bc

    % --- Calculation of the displacements a and reaction forces Q ---
    [a,Q]=solveq(K,f,bc);

```

```

% --- Calculating the total force vector f2= f + friction forces acting at the outer surface ---
f2=load2(Q,ndof,f,Dof);
[a,Q]=solveq(K,f2,bc);
ed=extract(Edof,a);
u=zeros(nel,1);

for q=1:nel
    % ---mixture rule ---
    E=4000e6*myb(q)+40e6*myc(q)+6e6*myt(q);
    v=0.3*myb(q)+0.35*myc(q)+0.47*myt(q);
    De=hooke(2,E,v);
    [es,et]=plani4saxi(Ex(q,:),Ey(q,:),[3 1 1],De,ed(q,:));
    % --- u: strain energy density ---
    u(q,1)=0.5*et*es';
end

% --- Fuzzy_rule=[1 0 0 0 0 0 0] = fuzzy rule number 1 is fulfilled ---
%    all the other rules are unfulfilled ----

for i=1:nel
    Fuzzy_rule=zeros(1,9);
    [mylow,myphys,myinc,mypath,mypoor,myhigh]=memberfunc_fuzzy(c(i,1),u(i,1));

    if myt(i,1)~=0

        if myhigh~=0&myphys~=0
            % --- R1 intramembranous ossification ---
            Fuzzy_rule(1,1)=1;
        end
        if myhigh~=0&myinc~=0
            % --- R2 intramembranous ossification ---
            Fuzzy_rule(1,2)=2;
        end

        if mypoor~=0&myinc~=0
            % --- R5 chondrogenesis ---
            Fuzzy_rule(1,5)=5;
        end
    end

    if myc(i,1)~=0
        if myhigh~=0&myphys~=0
            % --- R3 chondral ossification ---
            Fuzzy_rule(1,3)=3;
        end

        if myhigh~=0&myinc~=0
            % --- R4 chondral ossification ---
            Fuzzy_rule(1,4)=4;
        end

        if mylow~=0
            % --- R7 arthroply of cartilage ---
            Fuzzy_rule(1,7)=7;
        end
    end
end

```

```

        end

        if mypath~=0
            % --- R9 destruction of cartilage ---
            Fuzzy_rule(1,9)=9;
        end
    end

    if myb(i,1)~=0
        if mylow~=0
            % --- R6 arthropathy of bone ---
            Fuzzy_rule(1,6)=6;

            end
            if mypath~=0
                % --- R8 destruction of bone ---
                Fuzzy_rule(1,8)=8;
            end
        end

        [mybel,mycel,mytel]=fuzzy_controller(Fuzzy_rule,myt(i,1),myc(i,1),myb(i,1),
            mylow,myphys,myinc,mypath,mypoor,myhigh);
        myb(i,1)=mybel;
        myt(i,1)=mytel;
        myc(i,1)=mycel;
    end
    save C:\member_1 myb myt myc;
end

% -----End-----%

% -----Calculation of the initial state of the degree of membership -----%
%     myb = the degree of membership for bone
%     myc = the degree of membership for cartilage
%     myt = the degree of membership for soft tissue (connective tissue)
% -----
nel=100;
myb=zeros(nel,1);
myc=zeros(nel,1);
myt=zeros(nel,1);

for elnum=1:50
    myt(elnum)=1;
end

for elnum=51:nel
    myb(elnum)=1;
end

save C:\initial_my_fuzzy myb myc myt

% -----End-----%

```

% -----Calculation of the osteogenic factor c -----%

function [c]=osteogenic_factor(Ex,Ey,nel,myb)

myb=myb*100; % ---- [%]
 Ex=Ex*1000; %---- [mm]
 Ey=Ey*1000; %---- [mm]
 c=zeros(nel,1);

for i=1:nel
 switch i
 case {1,11,21,31,41,51,61,71,81,91}
 % --- symmetry ---
 c(i,1)=0;
 case {10,20,30,40,50,60,70,80,90,100}
 case {92,93,94,95,96,97,97,98,99}
 otherwise
 xgrad=(myb(i+1,1)-myb(i,1))/0.1; %----- $\Delta x = 0.1$ mm
 ygrad=(myb(i,1)-myb(i+10,1))/0.1; %----- $\Delta x = 0.1$ mm
 cgrad=[xgrad ygrad];
 c(i,1)=norm(cgrad);
 end
end

c(10,1)=0.5*(c(9,1)+c(19,1));
 c(20,1)=(1/3)*(c(9,1)+c(19,1)+c(29,1));
 c(30,1)=(1/3)*(c(19,1)+c(29,1)+c(39,1));
 c(40,1)=(1/3)*(c(29,1)+c(39,1)+c(49,1));
 c(50,1)=(1/3)*(c(39,1)+c(49,1)+c(59,1));
 c(60,1)=(1/3)*(c(49,1)+c(59,1)+c(69,1));
 c(70,1)=(1/3)*(c(59,1)+c(69,1)+c(79,1));
 c(80,1)=(1/3)*(c(69,1)+c(79,1)+c(89,1));
 c(90,1)=0.5*(c(89,1)+c(79,1));
 c(92,1)=(1/3)*(c(81,1)+c(82,1)+c(83,1));
 c(93,1)=(1/3)*(c(82,1)+c(83,1)+c(84,1));
 c(94,1)=(1/3)*(c(83,1)+c(84,1)+c(85,1));
 c(95,1)=(1/3)*(c(84,1)+c(85,1)+c(86,1));
 c(96,1)=(1/3)*(c(85,1)+c(86,1)+c(87,1));
 c(97,1)=(1/3)*(c(86,1)+c(87,1)+c(88,1));
 c(98,1)=(1/3)*(c(87,1)+c(88,1)+c(89,1));
 c(99,1)=(1/3)*(c(88,1)+c(89,1)+c(90,1));
 c(100,1)=(1/3)*(c(99,1)+c(89,1)+c(90,1));

% -----End -----%

%----- Calculation of the degree of membership for the fuzzy sets-----%
% mechanical stimulus u \rightarrow mylow,myphys,myinc,mypath
% the osteogenic factor c \rightarrow mypoor,myhigh
%-----

function [mylow,myphys,myinc,mypath,mypoor,myhigh]=memberfunc_fuzzy(c,u)
 u=u/1000;

```

mylow=0;
myphys=0;
myinc=0;
mypath=0;
mypoor=0;
myhigh=0;

% ---The membership functions are defined in Hofers article [10] ---

if 0.1<=u&0.4>u
    mylow=1;
end
if 0.4<=u&0.6>u
    mylow=-5*u+3;
end
if 0.4<=u&0.6>u
    myphys=5*u-2;
end
if 0.6<=u&1.8>u
    myphys=1;
end
if 1.8<=u&2.2>=u
    myphys=-2.5*u+5.5;
end
if 1.8<=u&2.2>u
    myinc=2.5*u-4.5;
end
if 2.2<=u&20>u
    myinc=1;
end

if 20<=u&55>u
    myinc=-0.0286*u+1.5730;
end

if 20<=u&55>u
    mypath=0.0286*u-0.5720;
end
if 55<=u
    mypath=1;
end

if 0<=c&0.7>c
    mypoor=1;
end
if 0.7<=c&8>=c
    mypoor=-0.137*c+1.0960;
end
if 0.7<=c&8>c
    myhigh=0.137*c-0.0959;
end
if 8<=c
    myhigh=1;
end

% -----End -----%

```

```
% -----The fuzzy controller -----%
```

```
function [mybel,mycel,mytel]=  
fuzzy_controller(Fuzzy_rule,myt,myc,myb,mylow,myphys,myinc,mypath,mypoor,myhigh)
```

```
dt=1; % --- [timestep=one day] ---
```

```
delta_b=0;  
delta_c=0;  
delta_t=0;
```

```
for j=1:9
```

```
    k=Fuzzy_rule(1,j);
```

```
    switch k
```

```
        case{1}
```

```
            % --- R1 intramembranous ossification, rate=1[%/day]---
```

```
            p=myt*myhigh*myphys;
```

```
            delta_t=delta_t-p*1*dt;
```

```
            delta_b=delta_b+p*1*dt;
```

```
        case{2}
```

```
            % --- R2 intramembranous ossification, rate=1[%/day]---
```

```
            p=myt*myhigh*myinc;
```

```
            delta_t=delta_t-p*1*dt;
```

```
            delta_b=delta_b+p*1*dt;
```

```
        case{3}
```

```
            % --- R3 chondral ossification, rate=2[%/day]---
```

```
            p=myc*myhigh*myphys;
```

```
            delta_c=delta_c-p*2*dt;
```

```
            delta_b=delta_b+p*2*dt;
```

```
        case{4}
```

```
            % --- R4 chondral ossification, rate=2[%/day]---
```

```
            p=myc*myhigh*myinc;
```

```
            delta_c=delta_c-p*2*dt;
```

```
            delta_b=delta_b+p*2*dt;
```

```
        case{5}
```

```
            % --- R5 chondrogenesis, rate=5[%/day]---
```

```
            p=myt*mypoor*myinc;
```

```
            delta_t=delta_t-p*5*dt;
```

```
            delta_c=delta_c+p*5*dt;
```

```
        case{6}
```

```
            % --- R6 arthroply of bone, rate=4[%/day]---
```

```
            p=myb*mylow;
```

```
            delta_b=delta_b-p*4*dt;
```

```
            delta_t=delta_t+p*4*dt;
```

```
        case{7}
```

```
            % --- R7 arthroply of cartilage, rate=8[%/day]---
```

```
            p=myc*mylow;
```

```
            delta_c=delta_c-p*8*dt;
```

```
            delta_t=delta_t+p*8*dt;
```

```
        case{8}
```

```
            % --- R8 destruction of bone, rate=10[%/day]---
```

```
            p=myb*mypath;
```

```
            delta_b=delta_b-p*10*dt;
```

```
            delta_t=delta_t+p*10*dt;
```

```
        case{9}
```

```

        % --- R9 destruction of cartilage, rate=20[%/day]---
        p=myc*mypath;
        delta_c=delta_c-p*20*dt;
        delta_t=delta_t+p*20*dt;
    otherwise
        % --- no change ---
    end
end
end

mybel=myb+delta_b/100; mytel=myt+delta_t/100; mycel=myc+delta_c/100;

% -----End -----%

% -----Calculation of the load vector f acting at the top and the boundary vector bc -----%

load C:\Geom_fuzzy

f=zeros(ndof,1);
p=2; % ---pressure = 2MPa ---

x1=0; x2=0.05;
f(2)=p*pi*(x1^2-x2^2);
x1=0.05; x2=0.15;
f(4)=p*pi*(x1^2-x2^2);
x1=0.15; x2=0.25;
f(6)=p*pi*(x1^2-x2^2);
x1=0.25; x2=0.35;
f(8)=p*pi*(x1^2-x2^2);
x1=0.35; x2=0.45;
f(10)=p*pi*(x1^2-x2^2);
x1=0.45; x2=0.55;
f(12)=p*pi*(x1^2-x2^2);
x1=0.55; x2=0.65;
f(14)=p*pi*(x1^2-x2^2);
x1=0.65; x2=0.75;
f(16)=p*pi*(x1^2-x2^2);
x1=0.75; x2=0.85;
f(18)=p*pi*(x1^2-x2^2);
x1=0.85; x2=0.9;
f(20)=p*pi*(x1^2-x2^2);

bc=[Dof(1,1) 0;
    Dof(12,1) 0;
    Dof(23,1) 0;
    Dof(34,1) 0;
    Dof(45,1) 0;
    Dof(56,1) 0;
    Dof(67,1) 0;
    Dof(78,1) 0;
    Dof(89,1) 0;
    Dof(100,1) 0;
    Dof(111,1) 0;
    Dof(11,1) 0;
    Dof(22,1) 0;
    Dof(33,1) 0;

```

```

Dof(44,1) 0;
Dof(55,1) 0;
Dof(66,1) 0;
Dof(77,1) 0;
Dof(88,1) 0;
Dof(99,1) 0;
Dof(110,1) 0;
Dof(121,1) 0;
Dof(121,2) 0;
Dof(120,2) 0];
bc=sort(bc);

save C:\load_bc_fuzzy f bc

%-----End-----%

%-----Calculation of the total force vector f2 -----%

function [f2]=load2(Q,ndof,f,Dof)

myfric_b=0.3;    % --- friction coefficient for bone ---
myfric_t=0.15;  % --- friction coefficient for soft tissue (connective tissue) ---
Ftemp=zeros(ndof,1);
Reacforce=zeros(11,2);

Reacforce(1,1)=Q(Dof(11,1));
Reacforce(1,2)=Dof(11,1);
Reacforce(2,1)=Q(Dof(22,1));
Reacforce(2,2)=Dof(22,1);
Reacforce(3,1)=Q(Dof(33,1));
Reacforce(3,2)=Dof(33,1);
Reacforce(4,1)=Q(Dof(44,1));
Reacforce(4,2)=Dof(44,1);
Reacforce(5,1)=Q(Dof(55,1));
Reacforce(5,2)=Dof(55,1);

Reacforce(6,1)=Q(Dof(66,1));
Reacforce(6,2)=Dof(66,1);
Reacforce(7,1)=Q(Dof(77,1));
Reacforce(7,2)=Dof(77,1);
Reacforce(8,1)=Q(Dof(88,1));
Reacforce(8,2)=Dof(88,1);
Reacforce(9,1)=Q(Dof(99,1));
Reacforce(9,2)=Dof(99,1);
Reacforce(10,1)=Q(Dof(110,1));
Reacforce(10,2)=Dof(110,1);
Reacforce(11,1)=Q(Dof(121,1));
Reacforce(11,2)=Dof(121,1);

for k=1:11
    switch k
        case {1,2,3,4,5}
            if Reacforce(k,1)<0
                Ftemp(Reacforce(k,2)+1)=abs(myfric_t*Reacforce(k,1));
            end
    end
end

```

```
    otherwise
      if Reacforce(k,1)<0
        Ftemp(Reacforce(k,2)+1)=abs(myfric_b*Reacforce(k,1));
      end
    end
  end

end
% --- f = force vector acting at the top of the model due to the pressure of 2MPa ---
f2=f+Ftemp;

%-----End-----%
```